Investigating the electrical conductivity and dielectric properties of compressed hydrocarbons using ultrafast terahertz radiation

Eric Sung, SLAC National Accelerator Laboratory
NIF & JLF Users Group Meeting
Feb. 12, 2025

The behavior of matter driven to warm dense matter conditions by dynamic laser compression are of interest to different areas of HED science

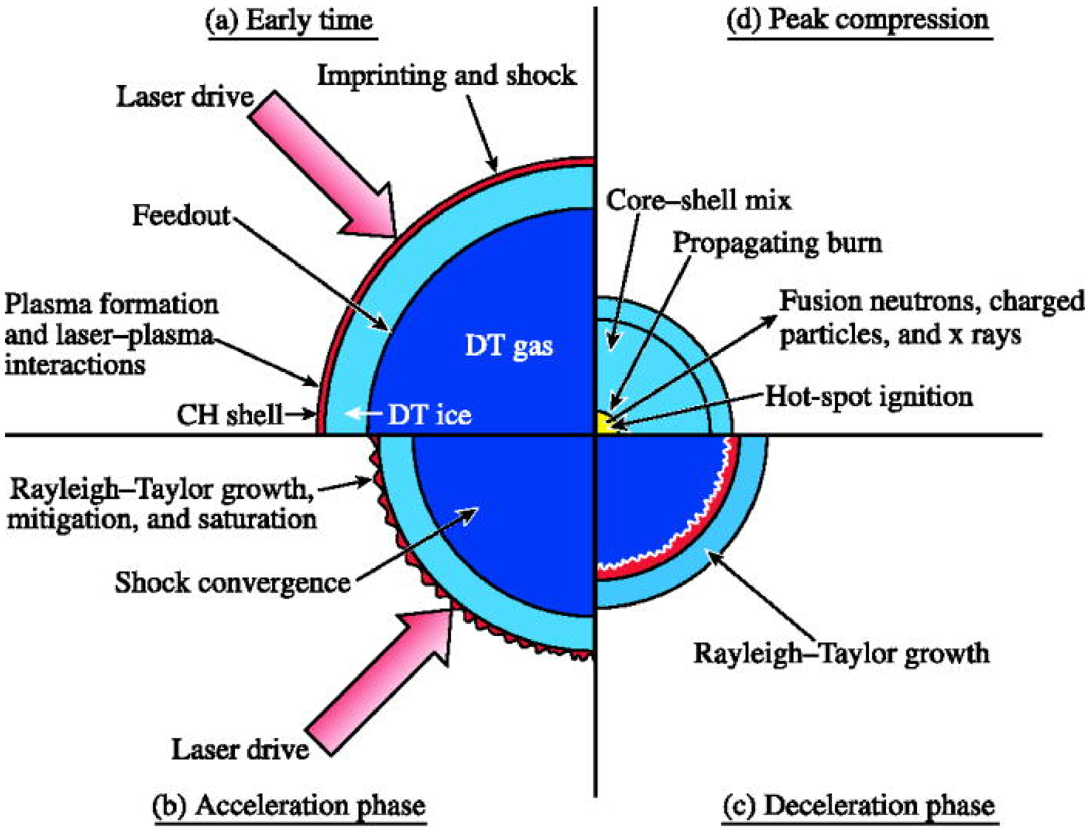

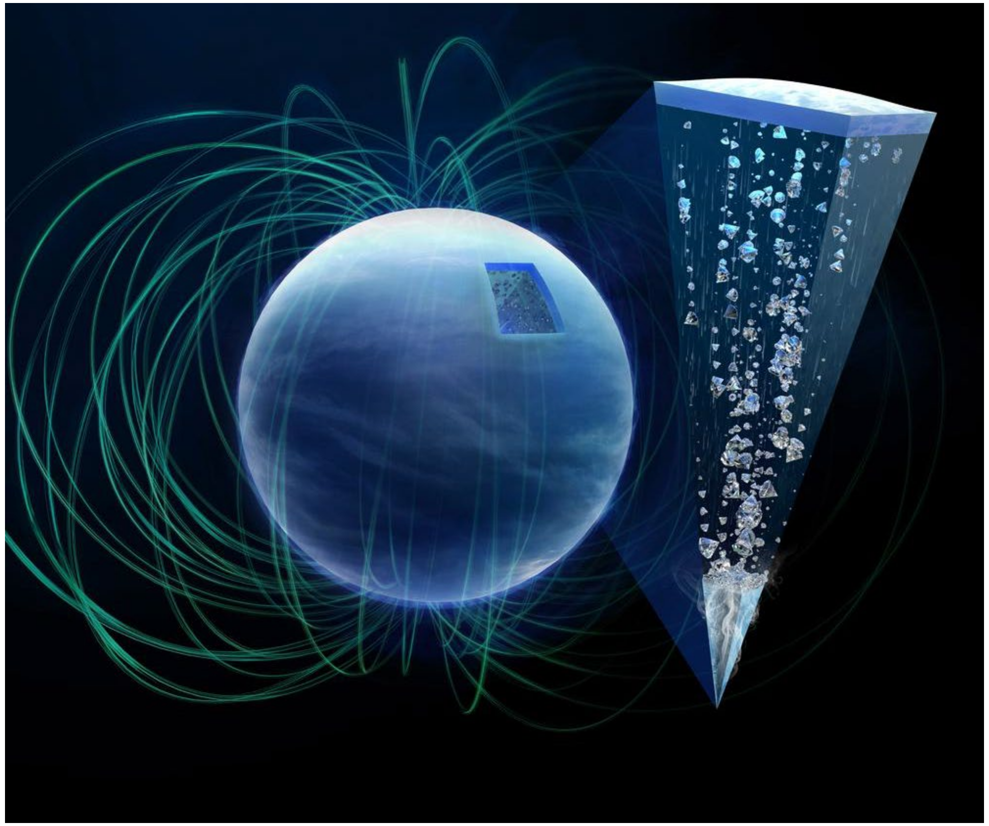

Understanding the behavior of compressed CH has important implications for IFE relevant physics and planetary models.

Craxton, et al., *Phys. Plasmas* **22** 110501 (2015)

Recent experiments at XFEL facilities have shown diamond formation when hydrocarbons are compressed to 100s GPa pressure and 1000s K temperature

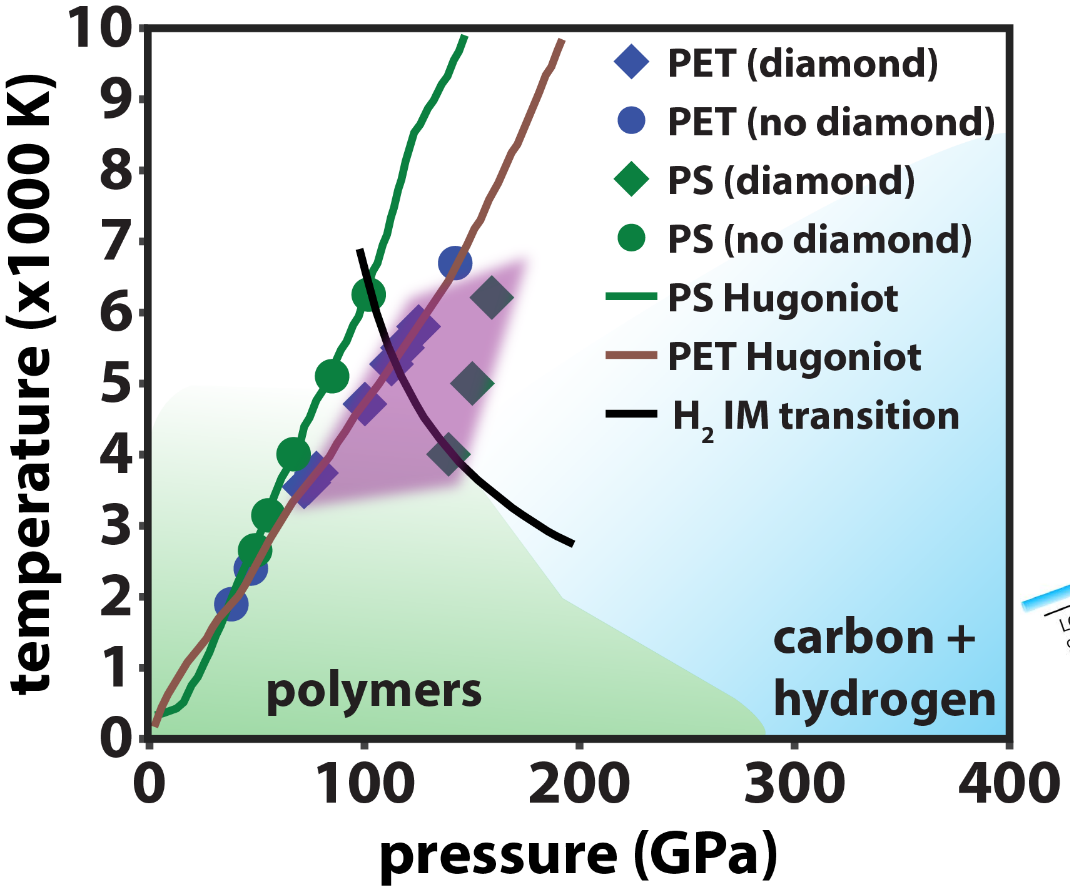

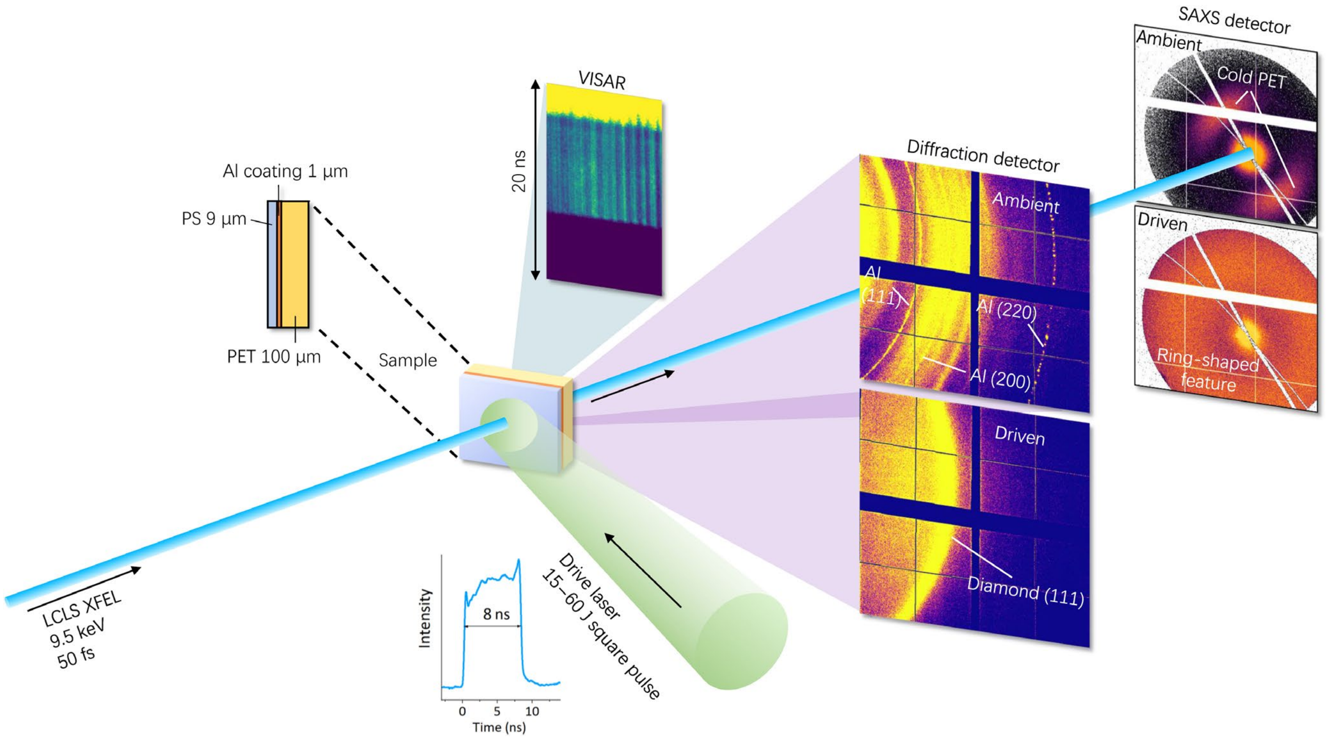

Direct experimental evidence of high conductivity material would confirm the presence of metallic H.

ersung@SLAC.stanford.edu

Kraus *et al.* *Nature Astronomy* **1**, 606 (2017)
He *et al.* *Sci. Adv.* **8**, eabo0617 (2022)
Kraus *et al.* *Phys. Rev. Res.* **5**, L022023, (2023)

Many different techniques have been used to measure the DC electrical conductivity of materials in the WDM regime

Optical Reflectivity

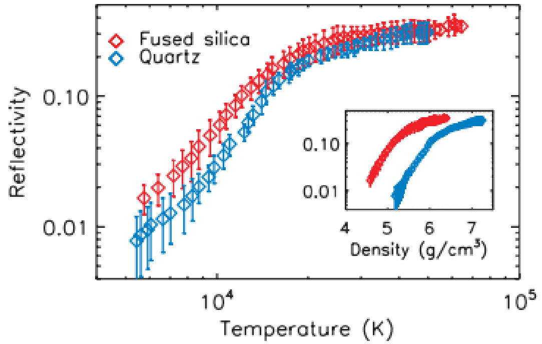

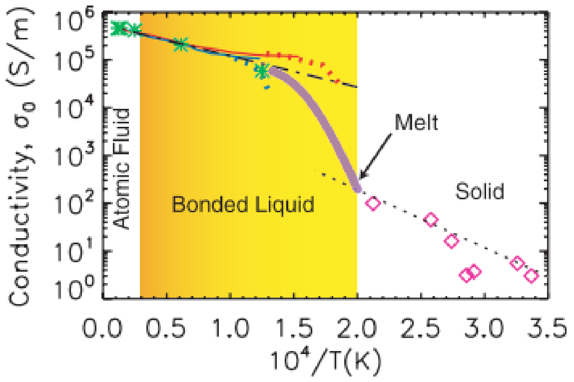

X-ray Thomson Scattering

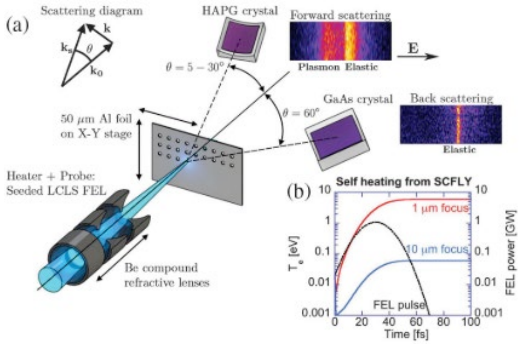

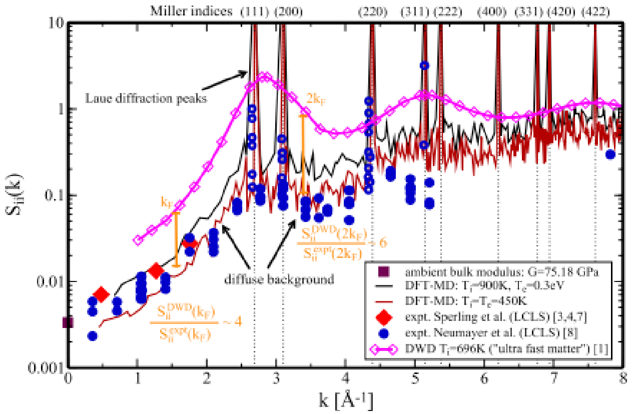

The ideal probe should also be sufficiently low frequency that it directly captures DC-like properties.

Hicks *et al.*, *Phys. Rev. Lett.* **97**(2), 025502 (2006)
Witte *et al.*, *Phys. Rev. E* **99**(4), 047201 (2019)
Sperling *et al.*, *Phys. Rev. Lett.* **115**(11), 115001 (2015)

Terahertz (THz) frequency radiation is a uniquely capable tool for investigating the conductivity of transient WDM

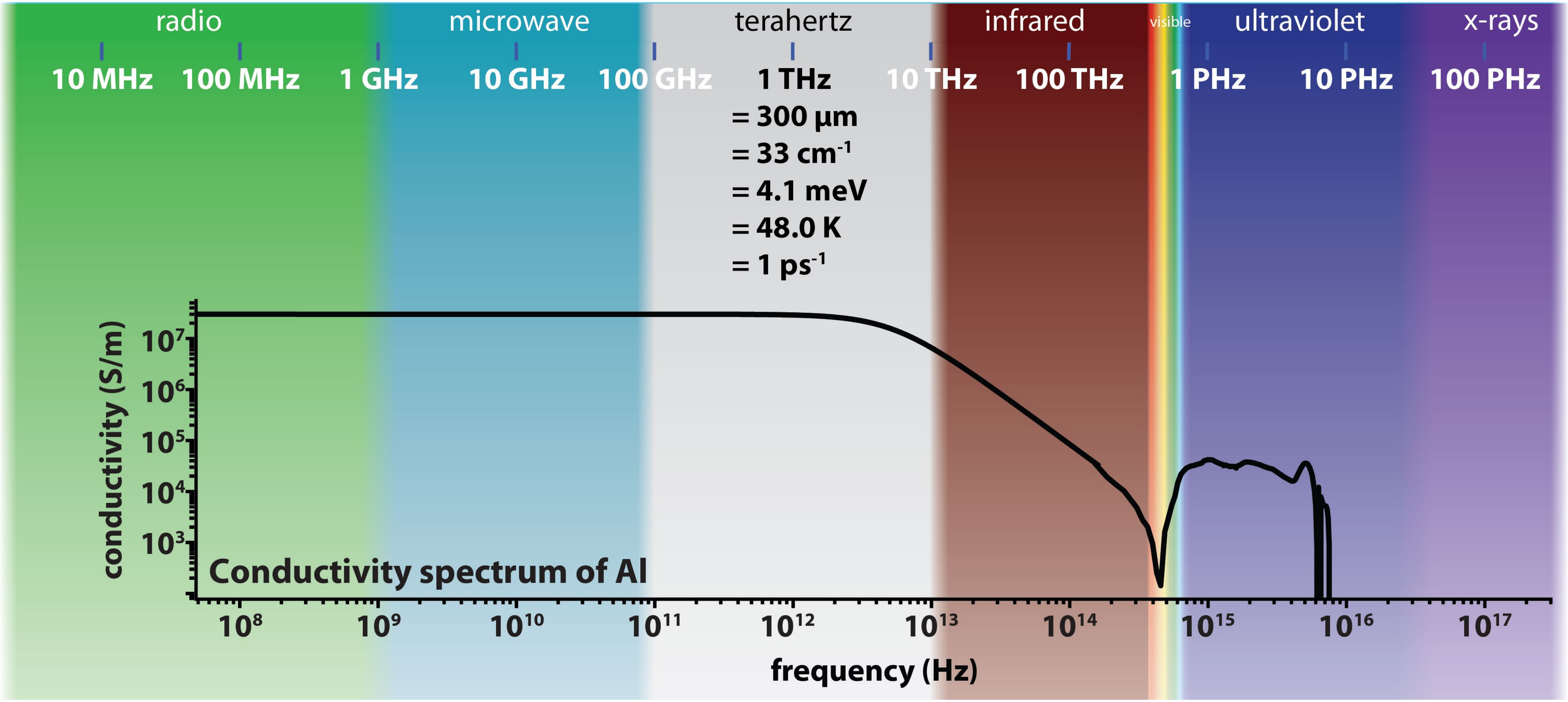

Terahertz (THz) frequency radiation is a uniquely capable tool for investigating the conductivity of transient WDM

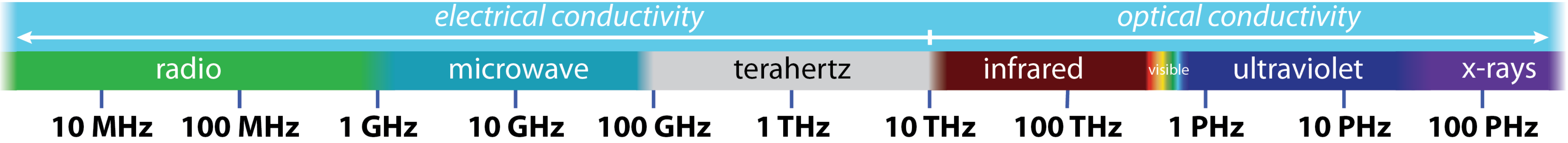

= 300 µm
= 33 cm^{-1}
= 4.1 meV
= 48.0 K
= 1 ps^{-1}

$$\frac{\nu_{\mathrm{THz}}}{\nu_e} \ll 1 \rightarrow \sigma(\nu_{\mathrm{THz}}) = \frac{\sigma_{\mathrm{DC}}}{1 - 2\pi i \frac{\nu_{\mathrm{THz}}}{\nu_e}} \sim \sigma_{\mathrm{DC}}$$

THz pulses are fast enough to probe ultrafast responses, but slow enough to measure DC properties

We record time-domain waveforms of the THz electric field, and these can be used to obtain the spectral response by numerical Fourier transformation

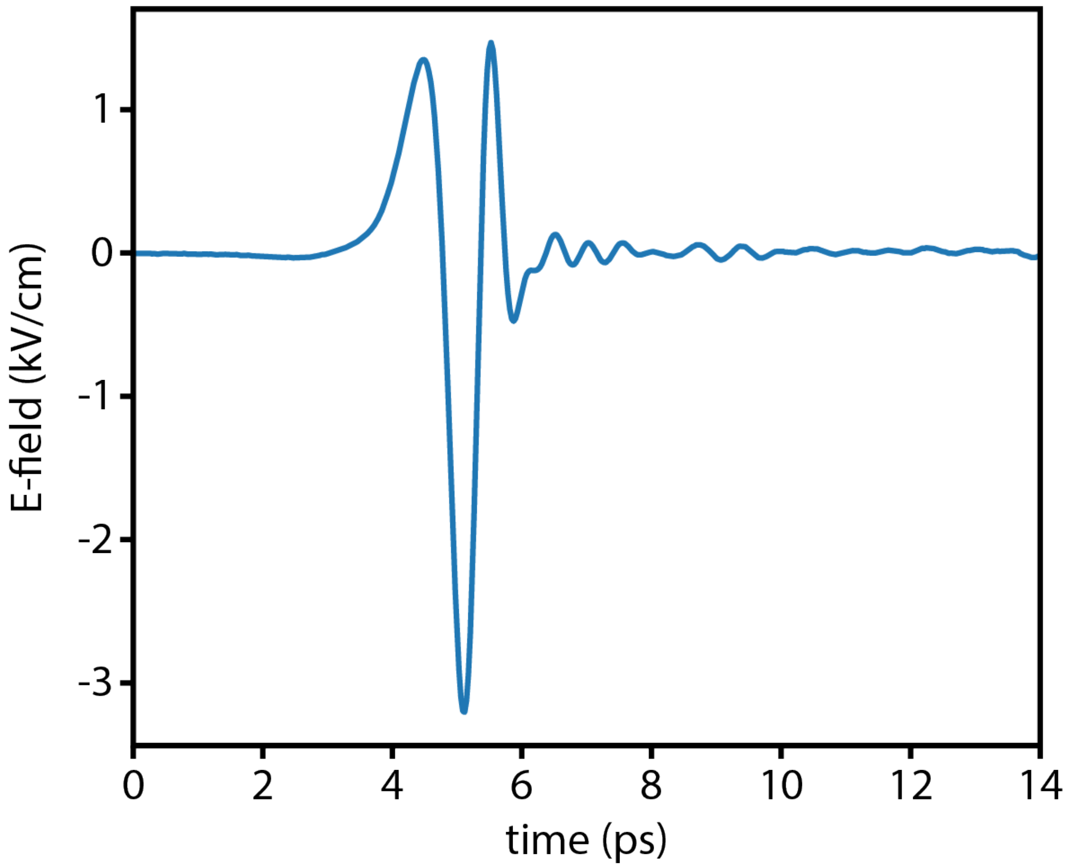

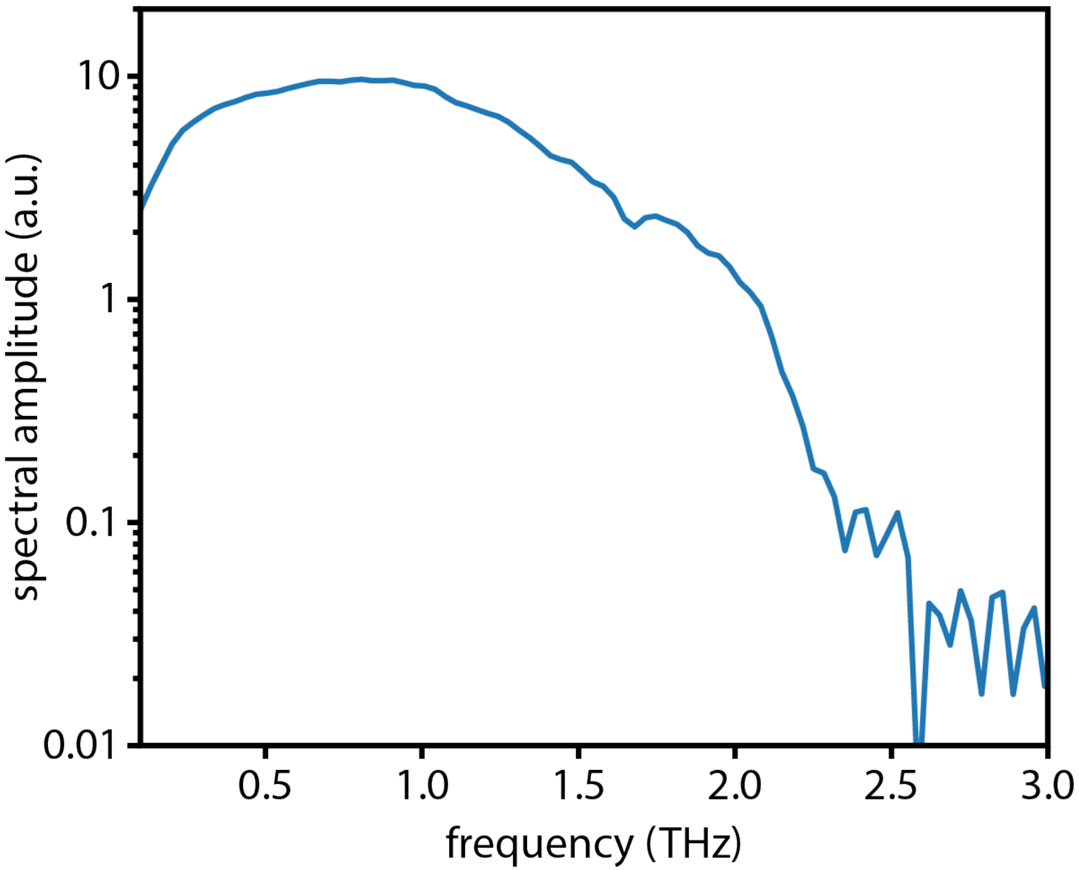

THz time-domain waveforms contains information about the frequency-dependent response of a material.

Minami *et al.*, *Appl. Phys. Lett.* **103**(5), 51103 (2013)
Noe *et al.*, *Opt. Express* **24**(26), 30328–30337 (2016)
Russell*, Ofori-Okai* *et al.*, *Opt. Express* **25**(14), 16140 (2017)
Ofori-Okai *et al.*, *Phys. of Plasmas* **31** 042711 (2024)

We performed experiments at the Jupiter Laser Facility to investigate the formation of metallic hydrogen during the compression of plastic to 100s GPa pressure

Experimental goals:

1. THz reflectivity of shocked **polystyrene (PS)**
   - No diamond formation under single shock
2. THz reflectivity of shocked **polyethylene terephthalate (PET)**
   - Between ~75-125 GPa, diamond formation
   - Above 110 GPa, expect hydrogen metallization

JLF Janus Lasers

Long pulse energy	= up to 775 J
Pulse duration	= 10-20 ns
Spot size	= 1 mm
Shot rate	= 2/hr

Short pulse energy	= 5 mJ
Duration	= 50 fs
Rep rate	= 10 Hz

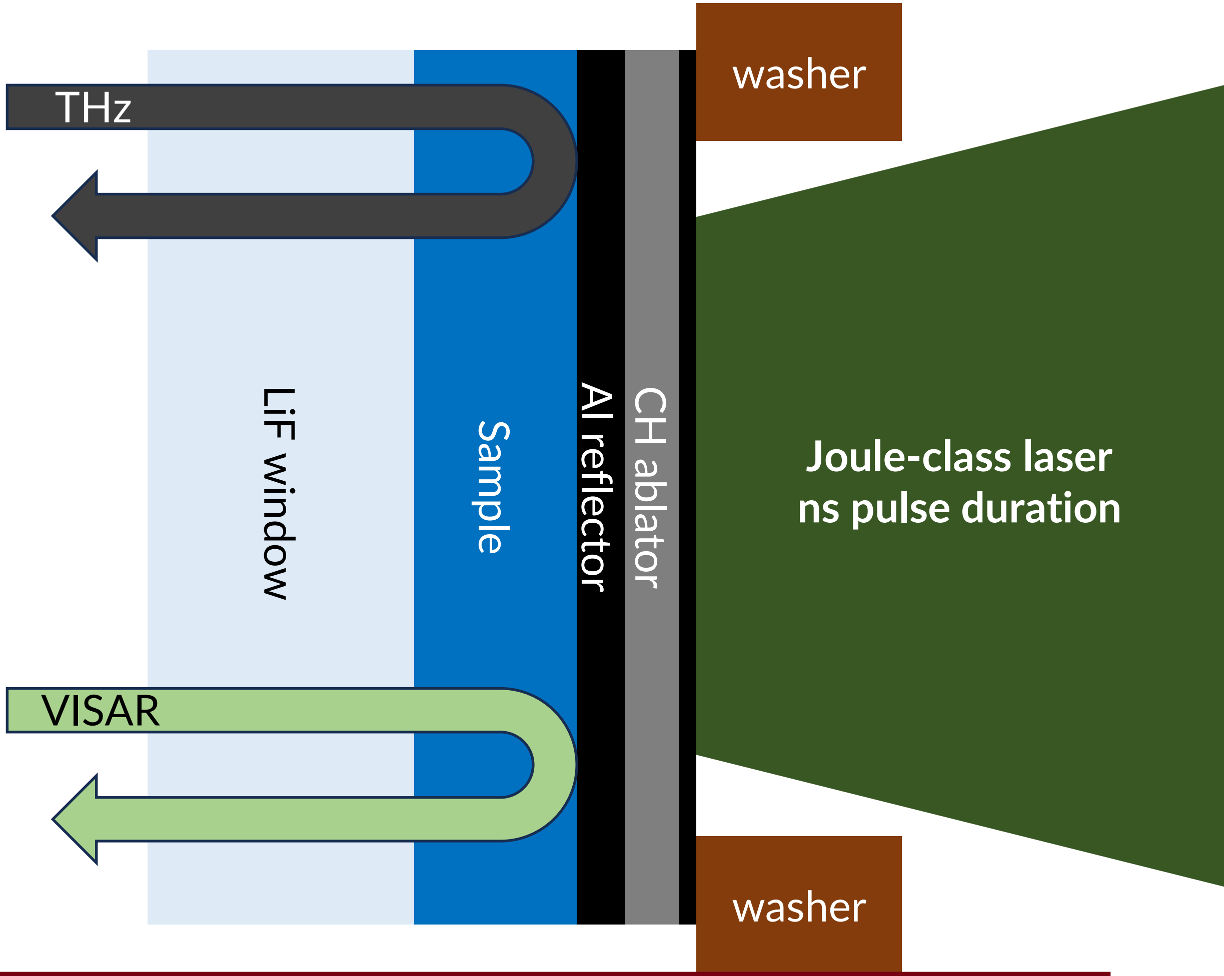

The recently upgraded high energy laser at JLF can shock large sample areas to high pressure.

Line VISARs were used to determine the shock transit time, and additional fiducials were used determine the arrival time of the THz pulse

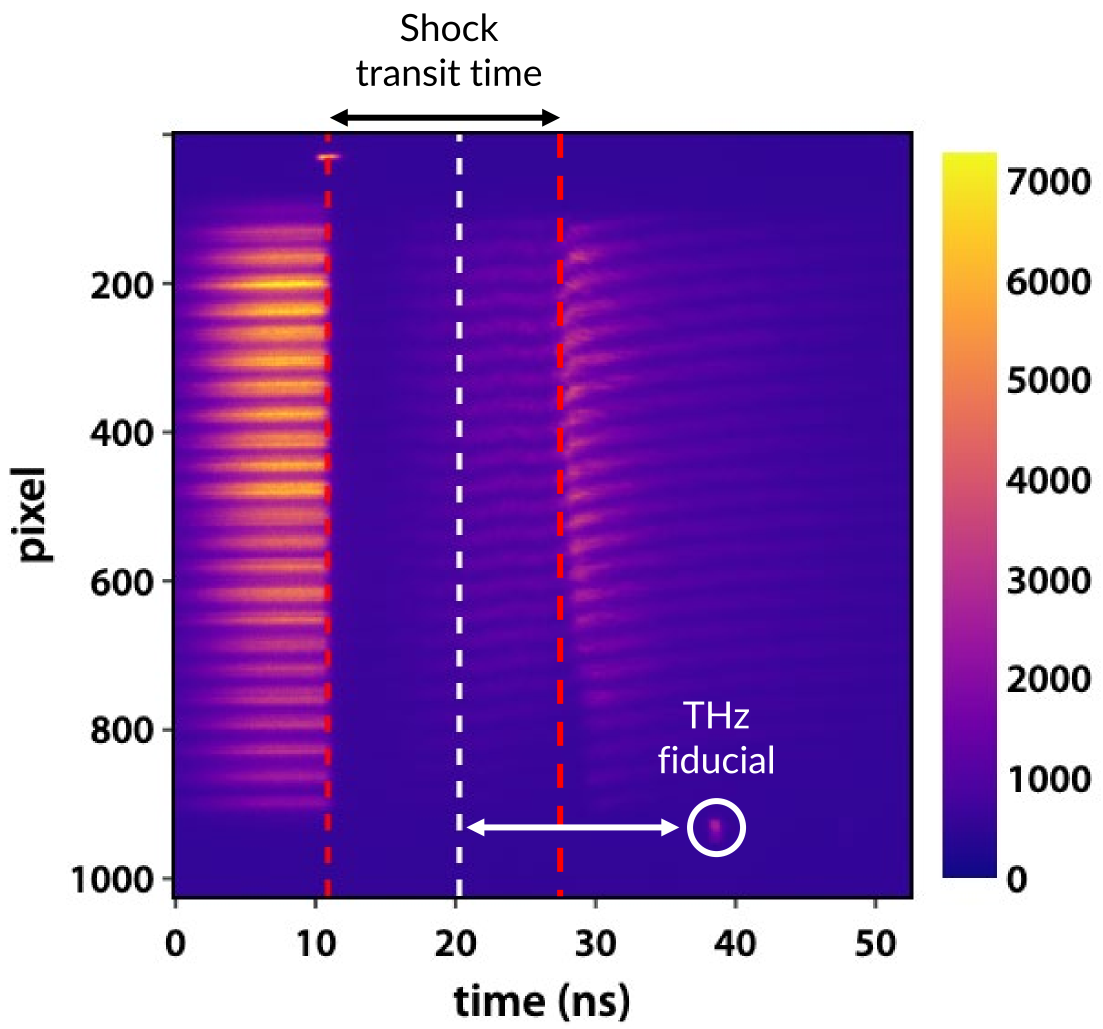

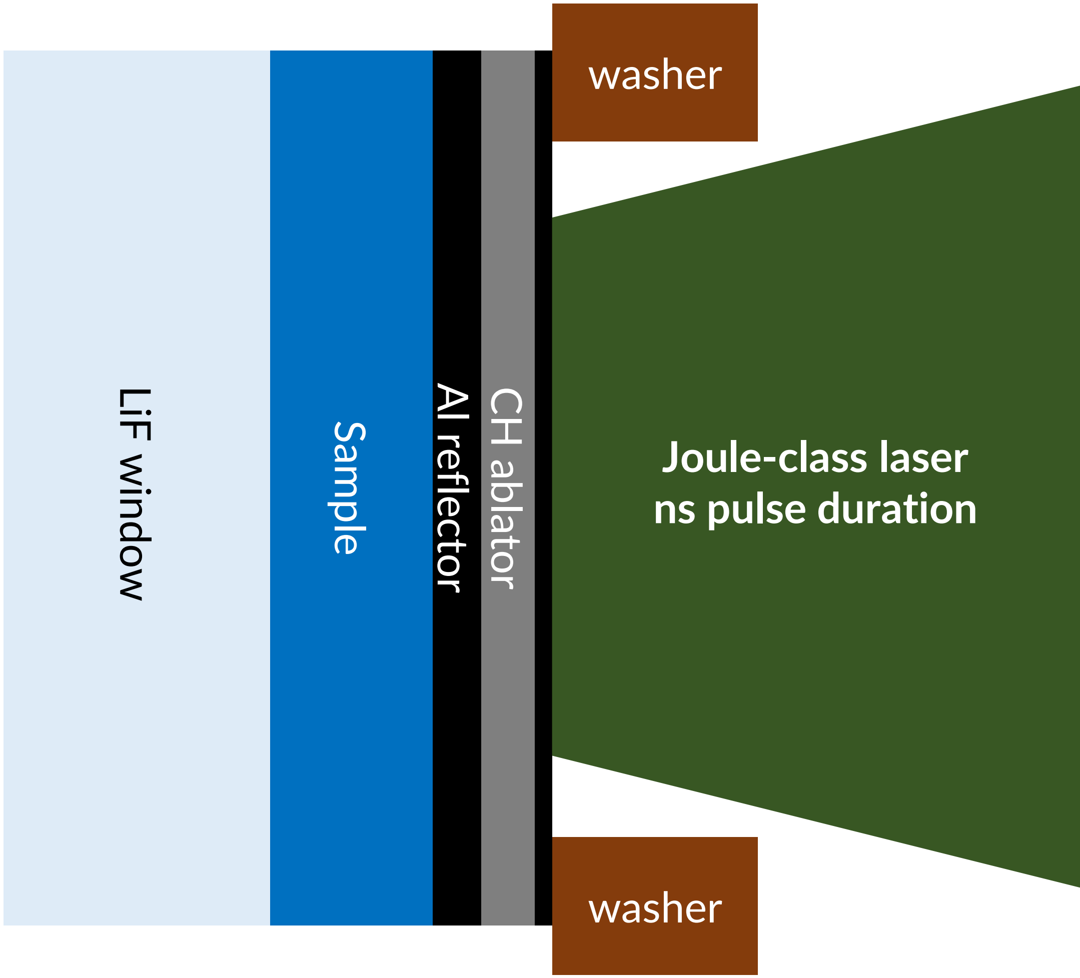

1D simulations of THz pulse reflecting at various interfaces within the target: Ambient plastic

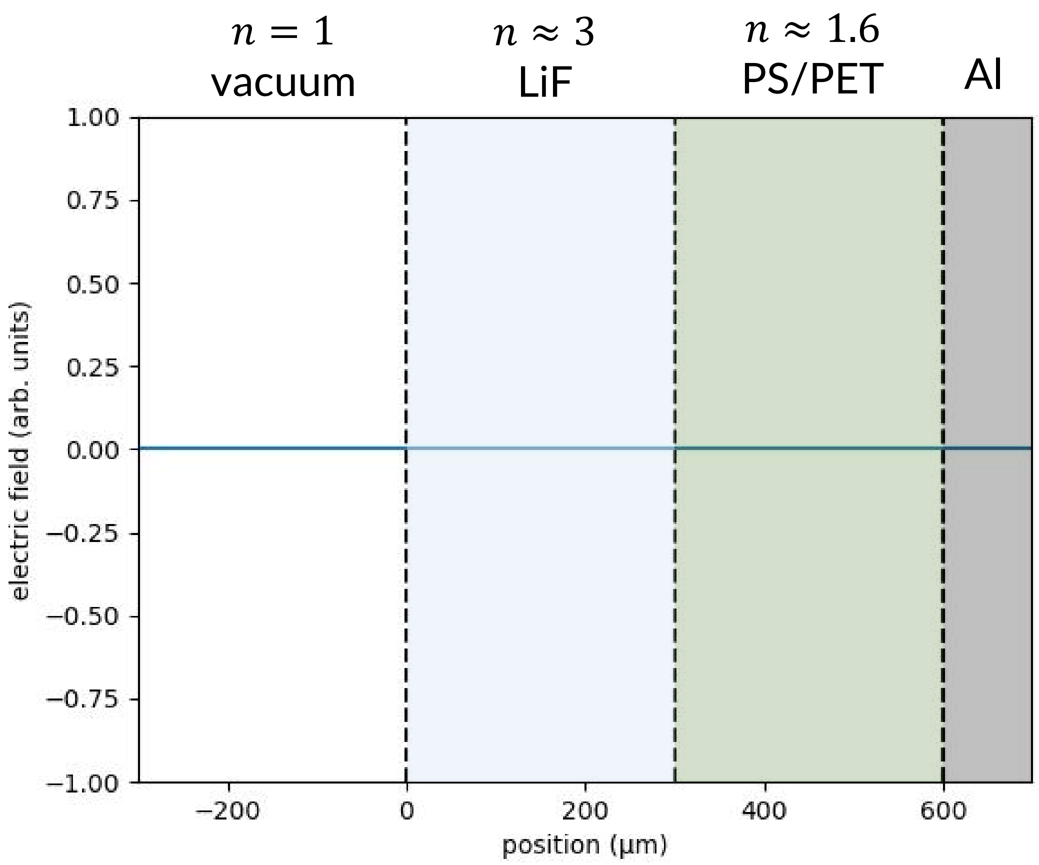

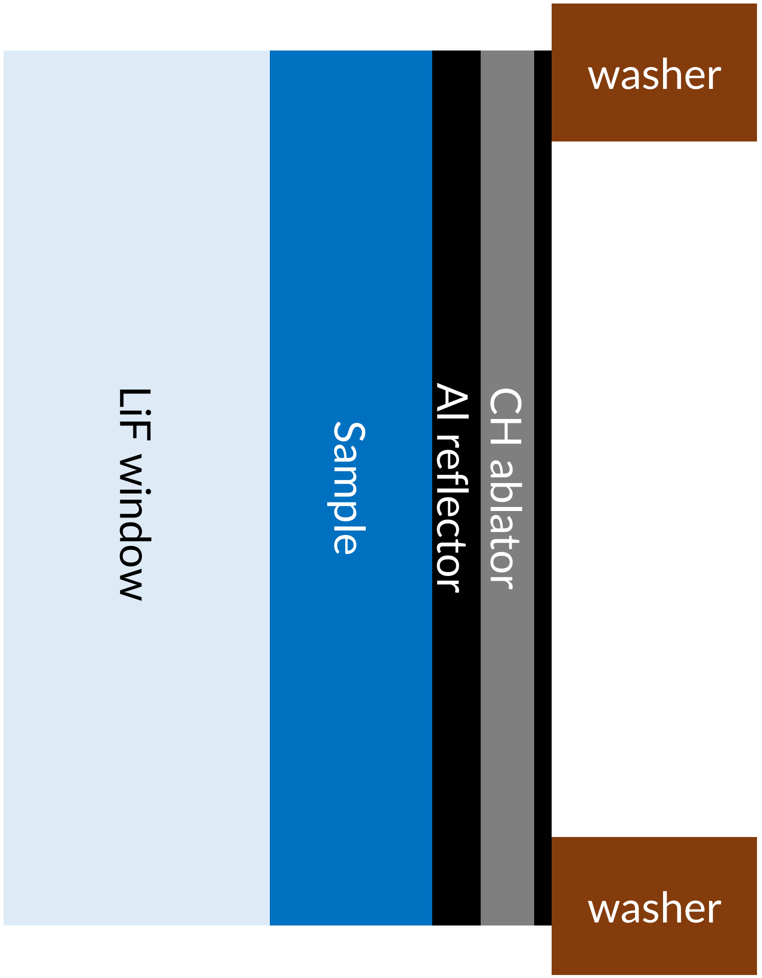

1D simulations of THz pulse reflecting at various interfaces within the target: Ambient plastic

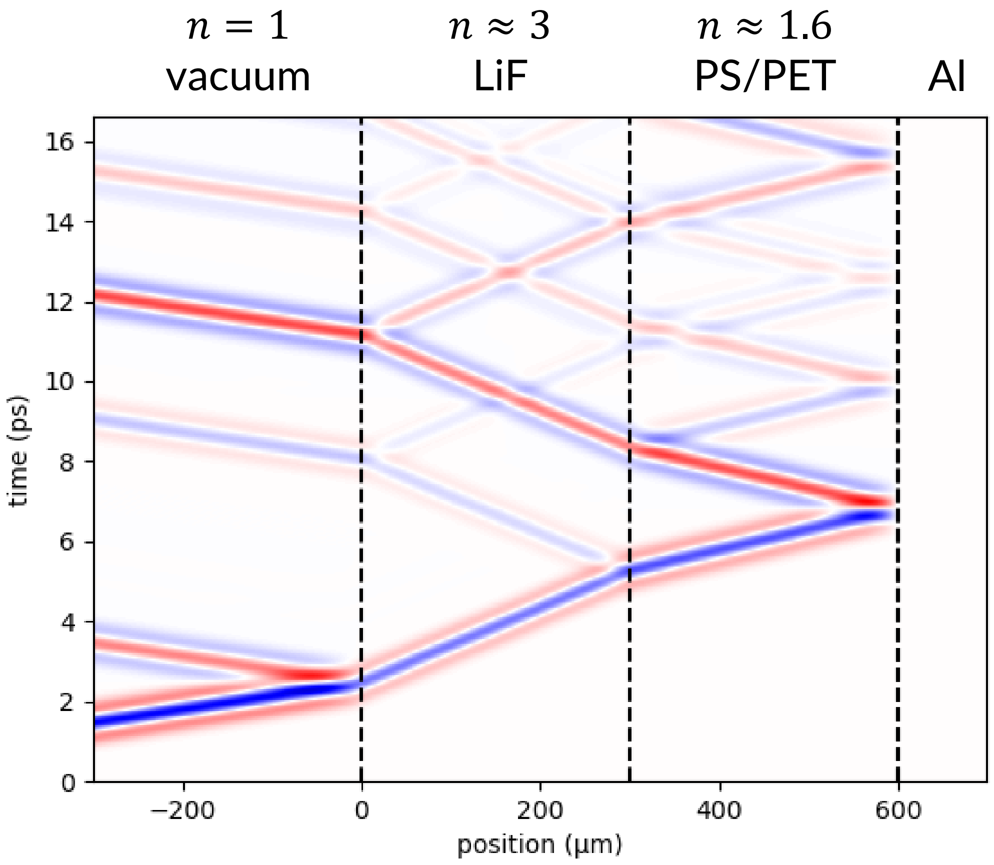

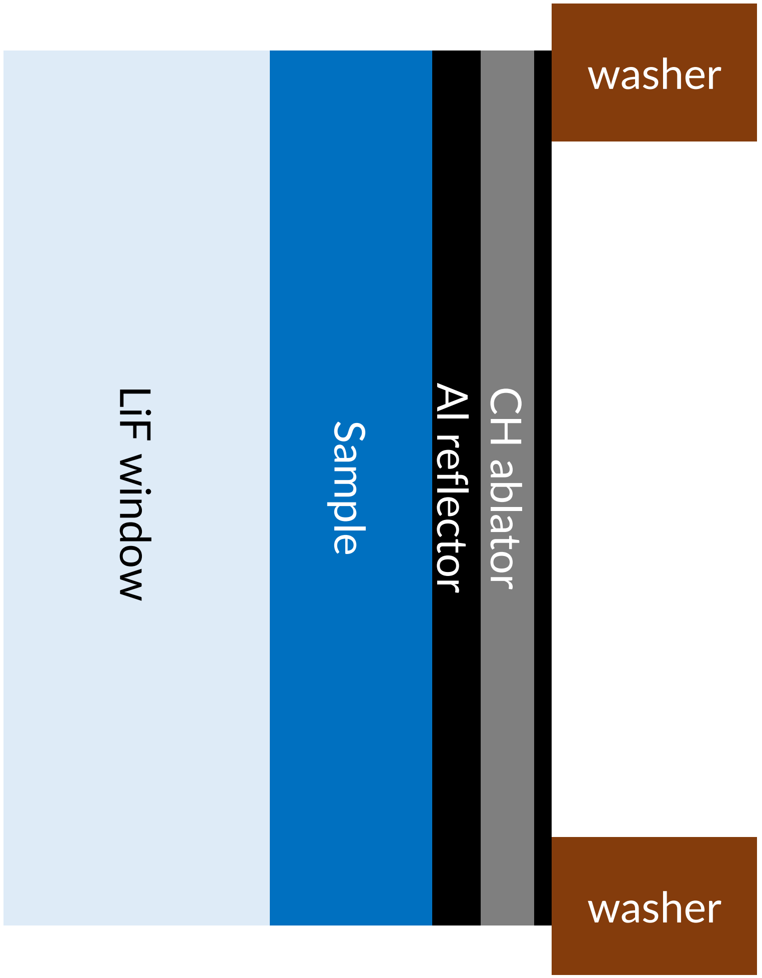

1D simulations of THz pulse reflecting at various interfaces within the target: Ambient plastic

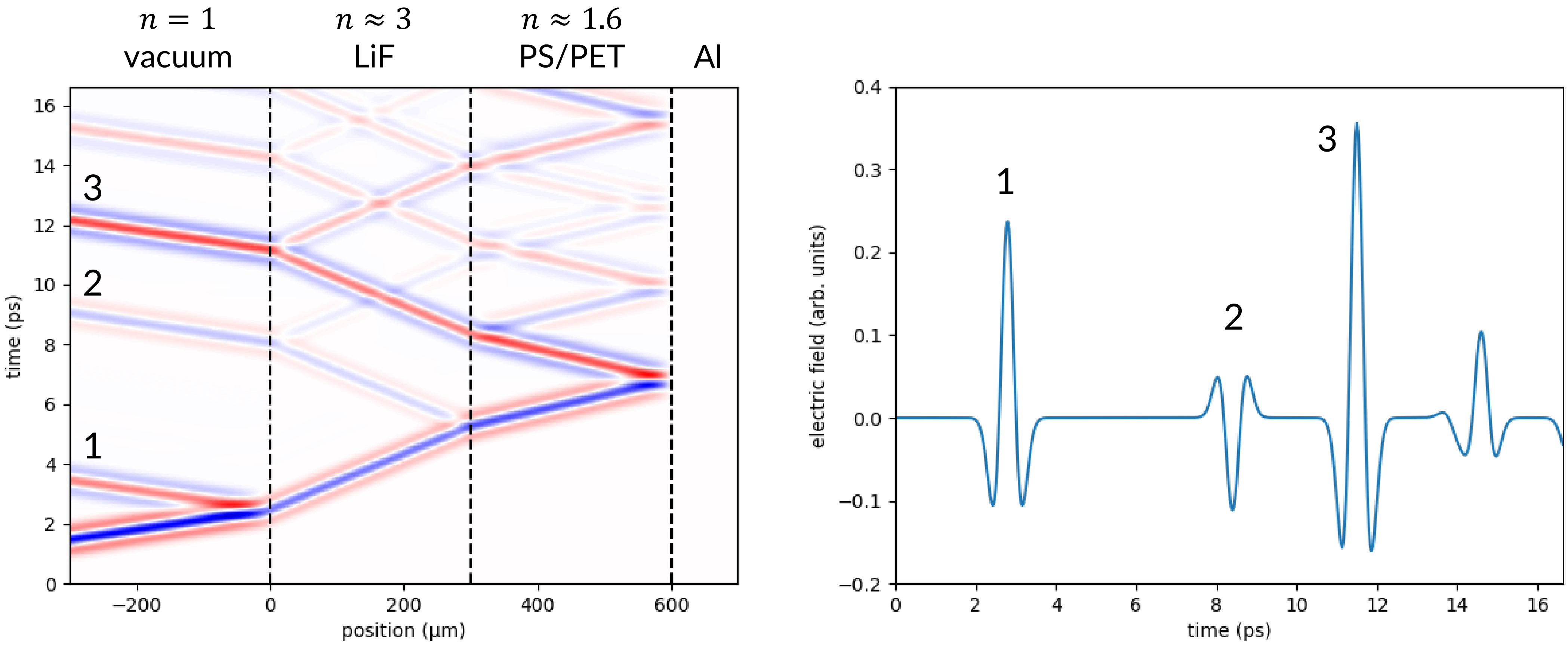

1. vacuum-LiF interface reflection
2. LiF-plastic interface reflection
3. plastic-Al interface reflection

1D simulations of THz pulse reflecting at various interfaces within the target: Shocked plastic, n ~ 4

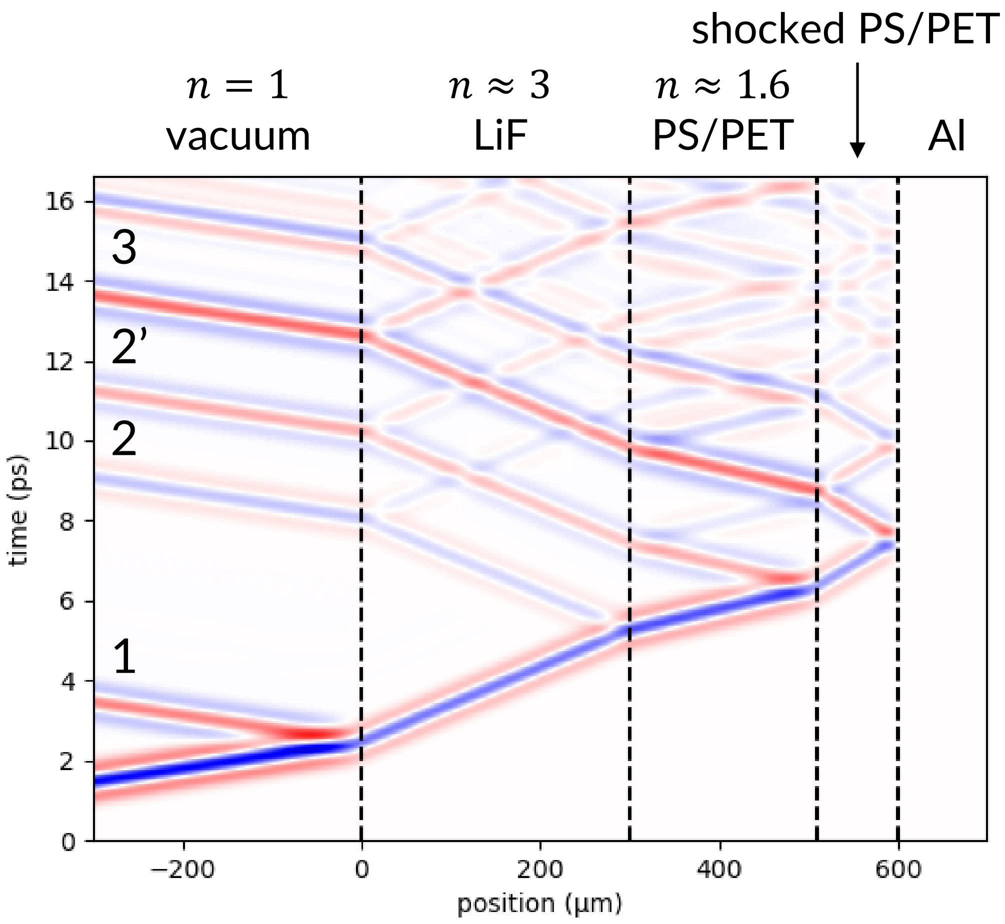

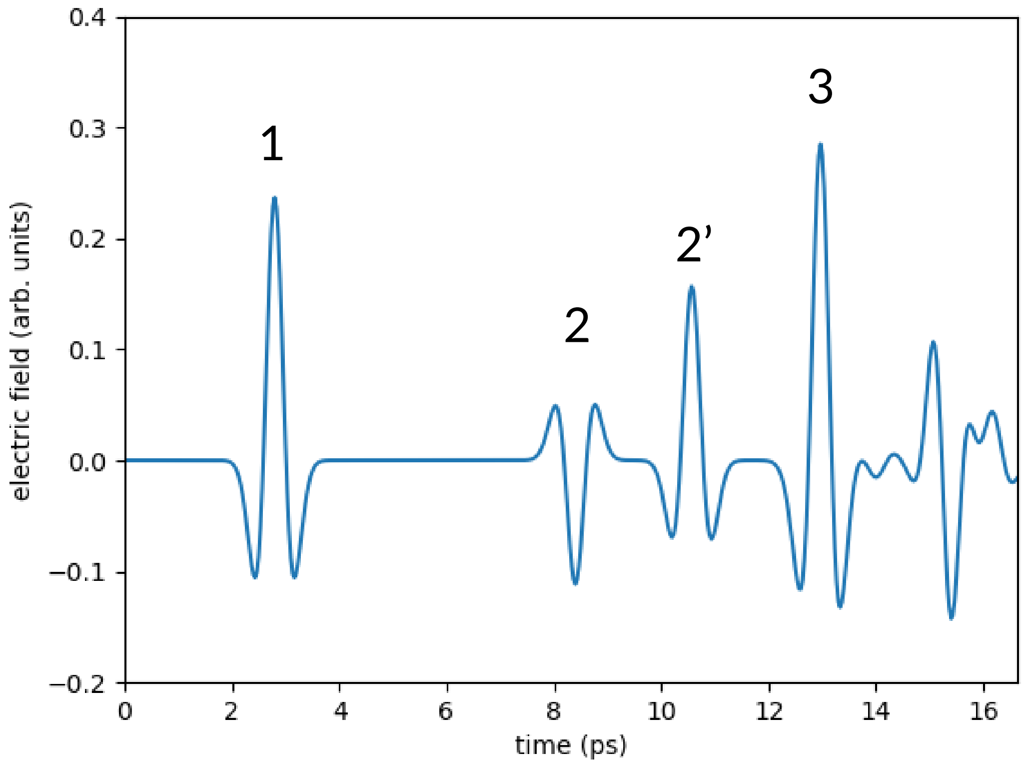

1. vacuum-LiF interface reflection
2. LiF-unshocked plastic interface reflection
2'. unshocked-shocked plastic interface reflection
3. plastic-Al interface reflection

1D simulations of THz pulse reflecting at various interfaces within the target: Shocked plastic, highly conductive

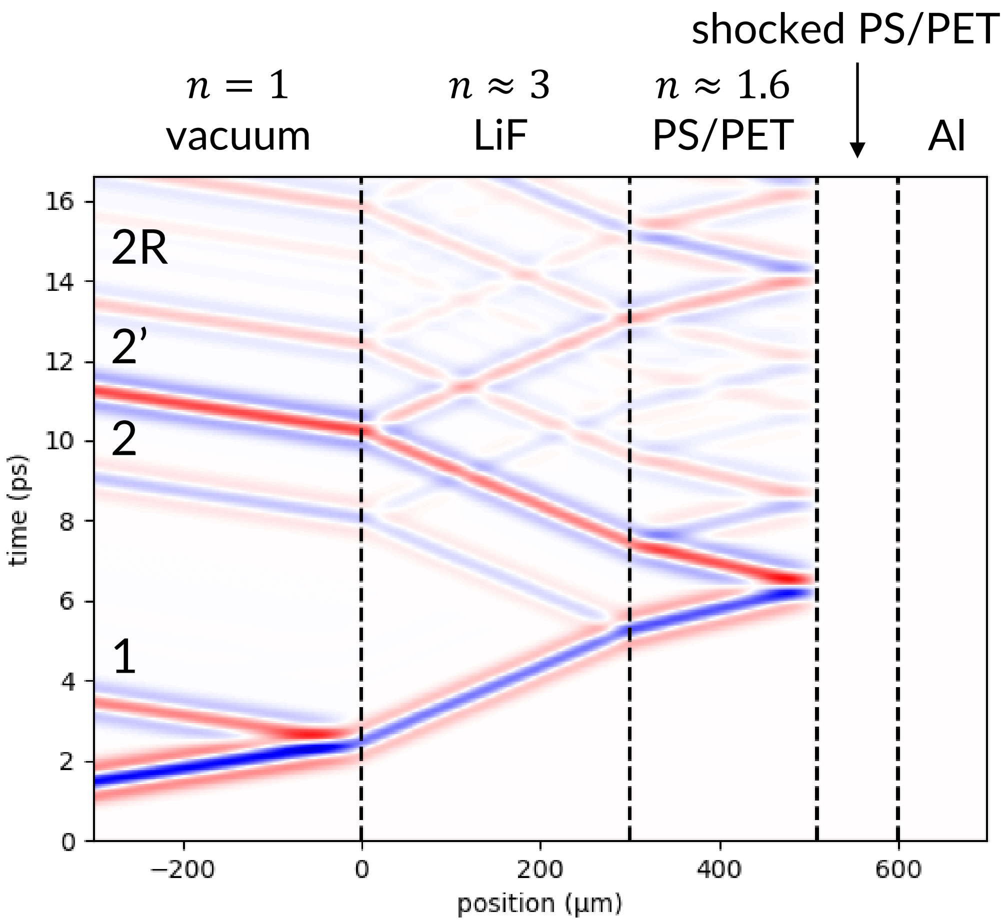

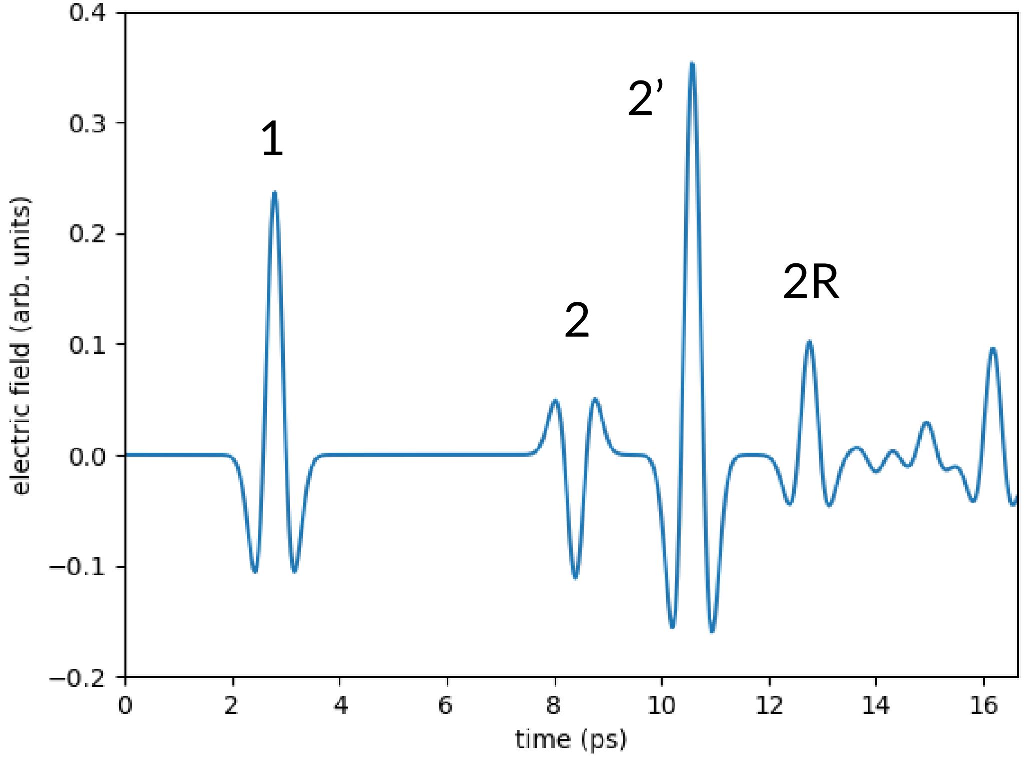

1. vacuum-LiF interface reflection
2. LiF-unshocked plastic interface reflection

2'. **unshocked-shocked plastic interface reflection**

2R. double roundtrip inside unshocked plastic

Time-domain waveform shows multiple THz pulses due to reflections at various interfaces within the target assembly

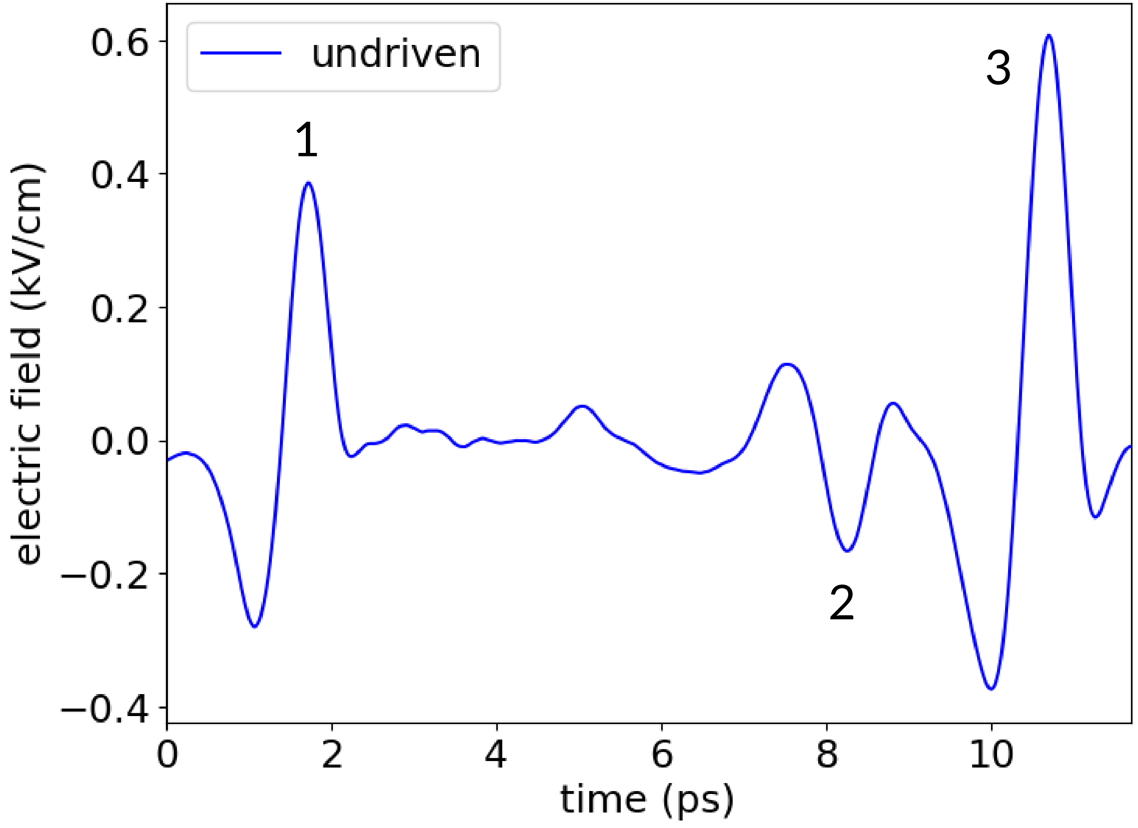

Polystyrene target assembly

Reflections occur when there is a significant change in the refractive index:

$$\tilde{r}_p = \frac{\tilde{n}_1 \cos(\theta_2) - \tilde{n}_2 \cos(\theta_1)}{\tilde{n}_1 \cos(\theta_2) + \tilde{n}_2 \cos(\theta_1)}$$

$\tilde{n}_1$= refractive index of layer 1
$\tilde{n}_2$= refractive index of layer 2

We observe reflections at:

1. vacuum-LiF interface
2. LiF-PS interface
3. PS-Al interface

The time-domain waveform can be decomposed to extract contributions from the various pulses arising from reflections at different interfaces

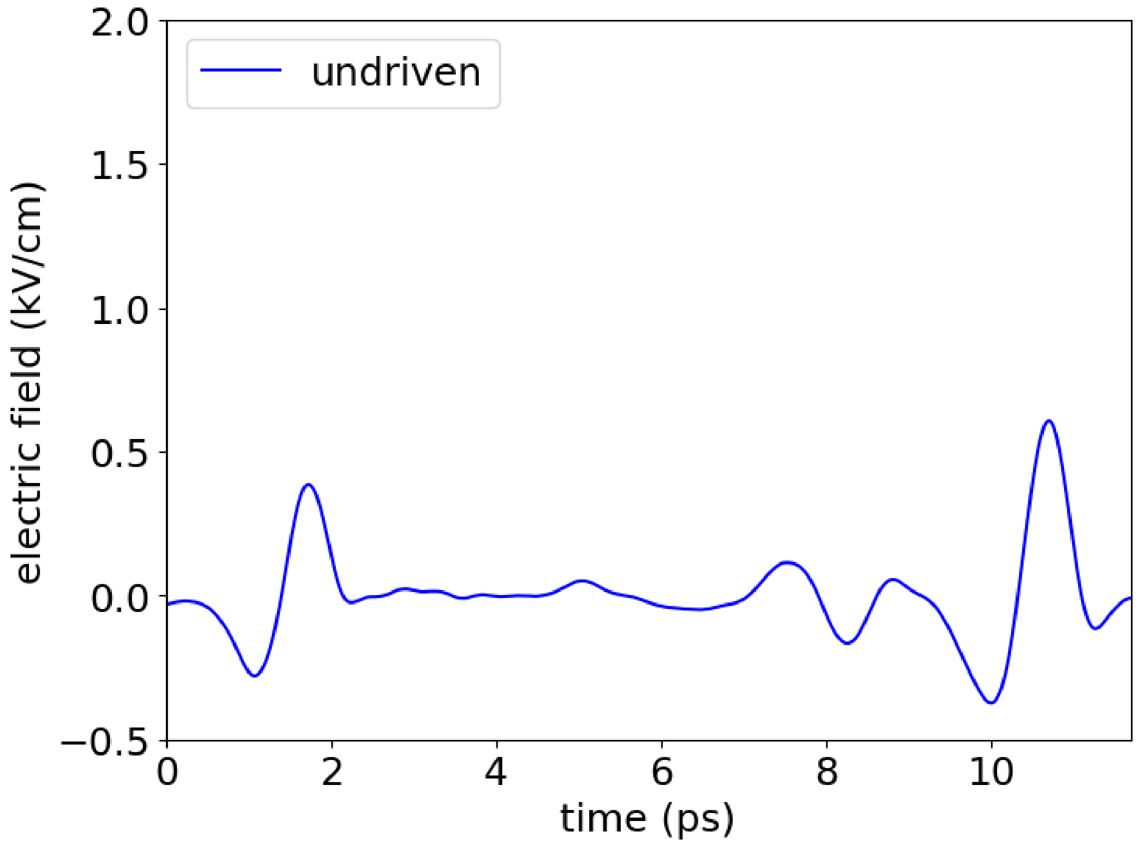

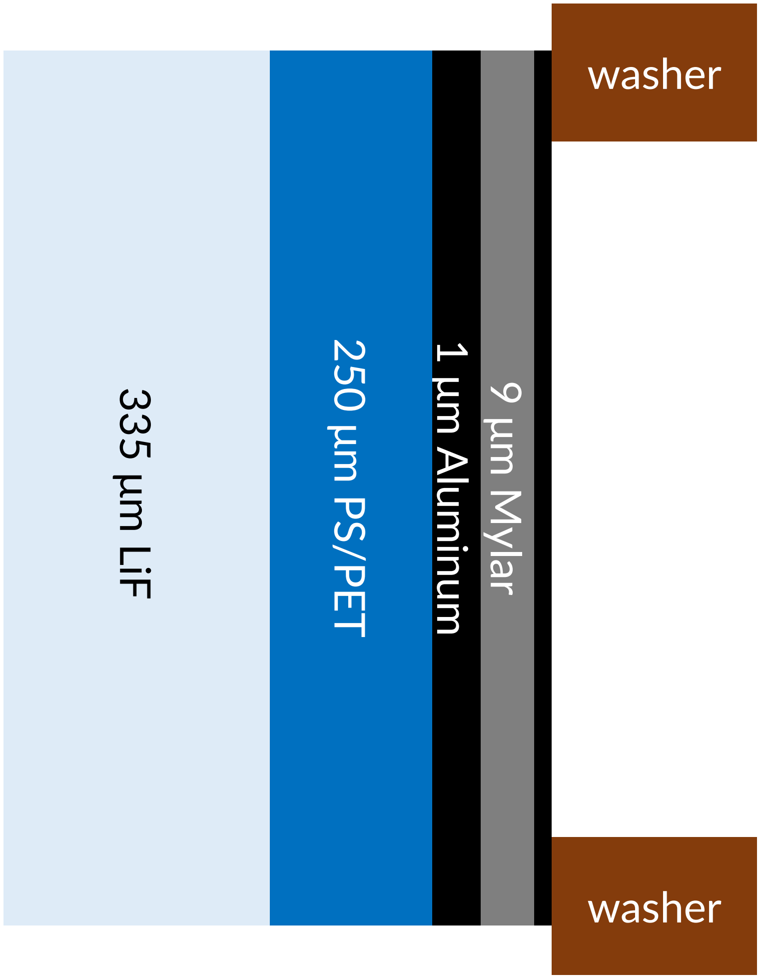

The time-domain waveform can be decomposed to extract contributions from the various pulses arising from reflections at different interfaces

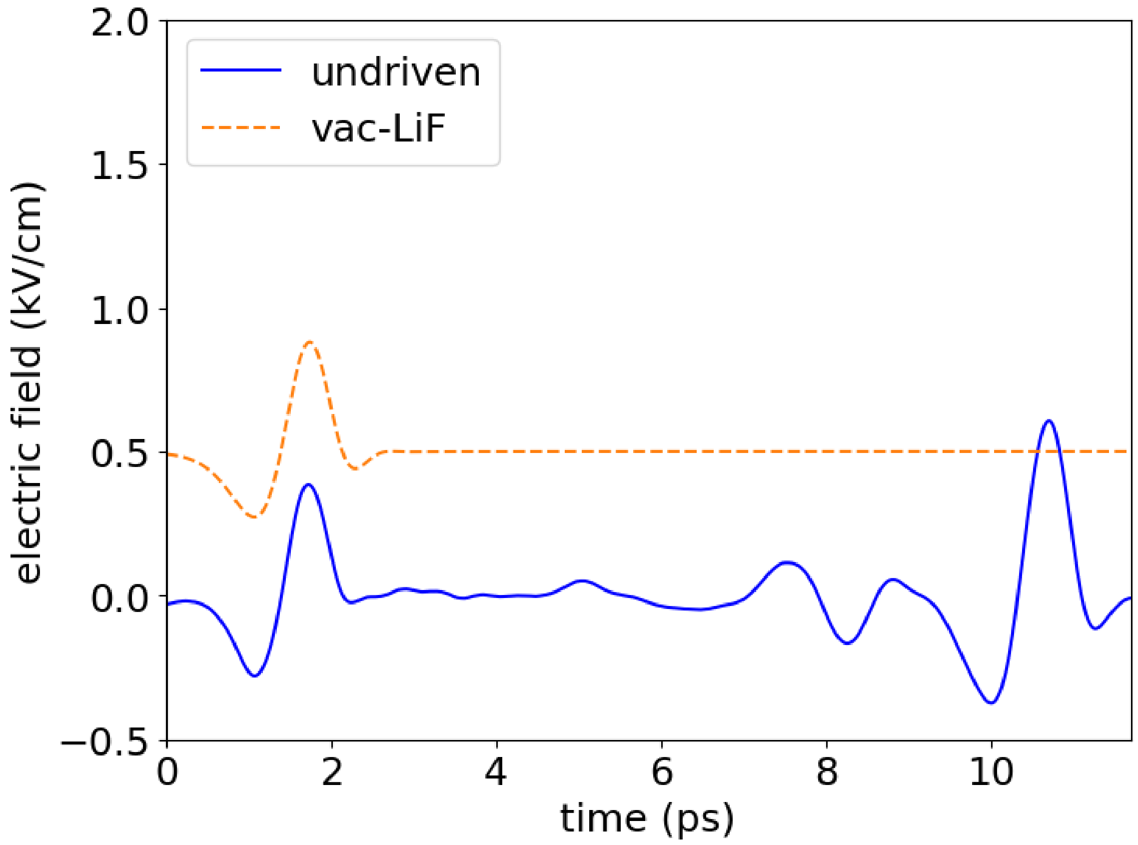

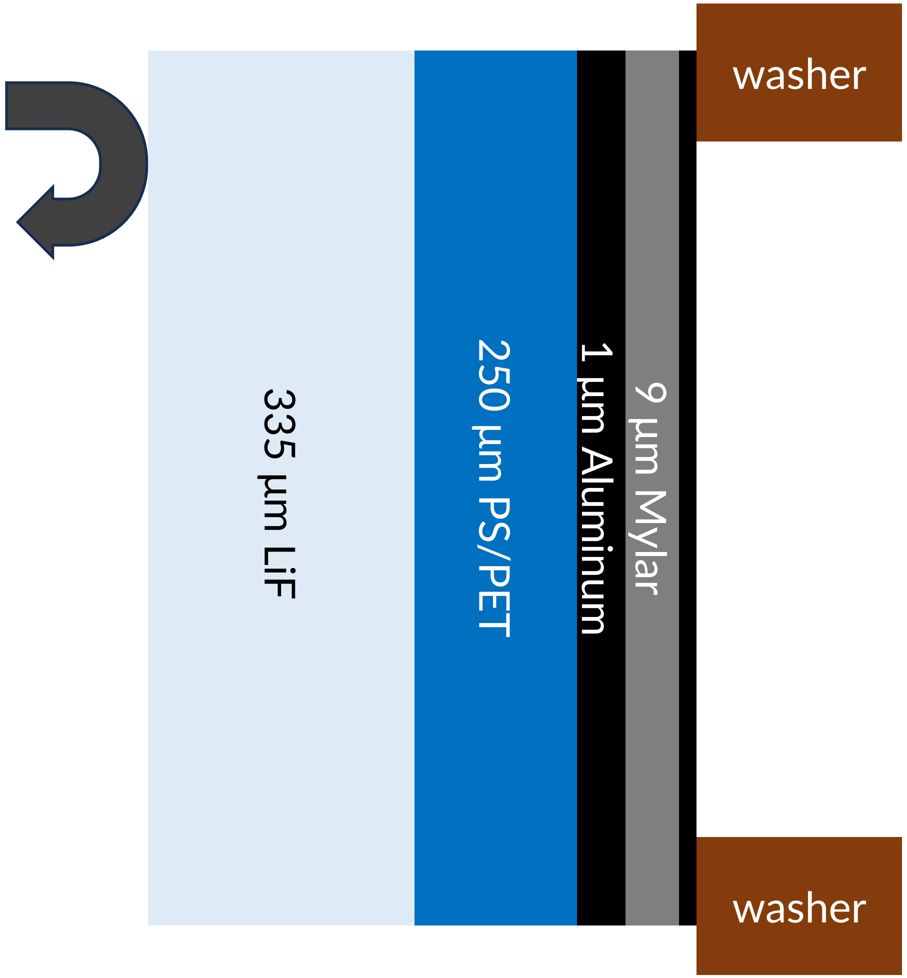

The time-domain waveform can be decomposed to extract contributions from the various pulses arising from reflections at different interfaces

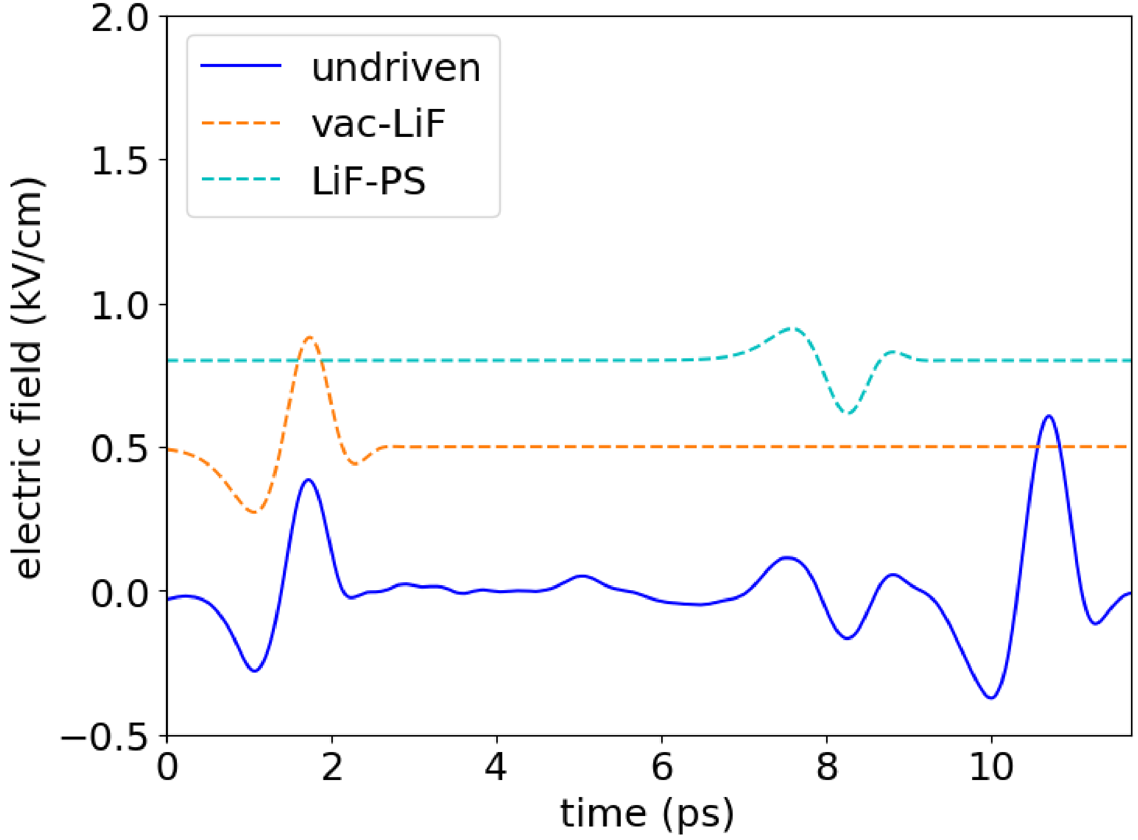

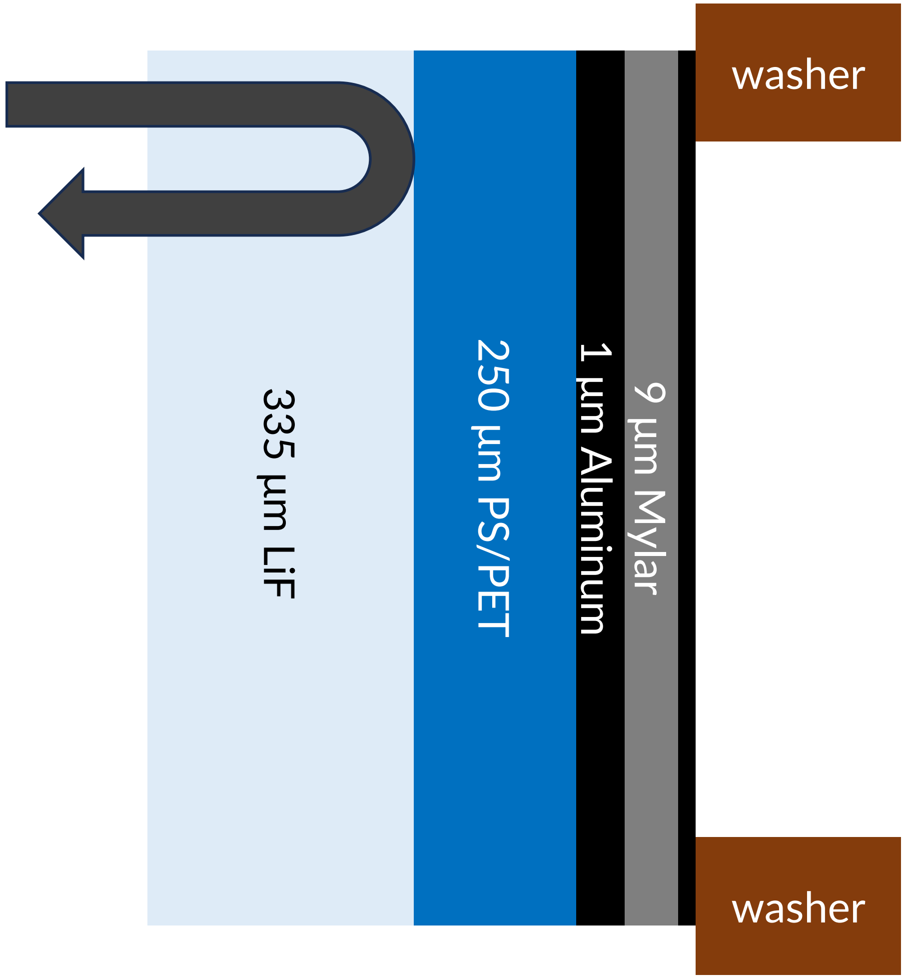

The time-domain waveform can be decomposed to extract contributions from the various pulses arising from reflections at different interfaces

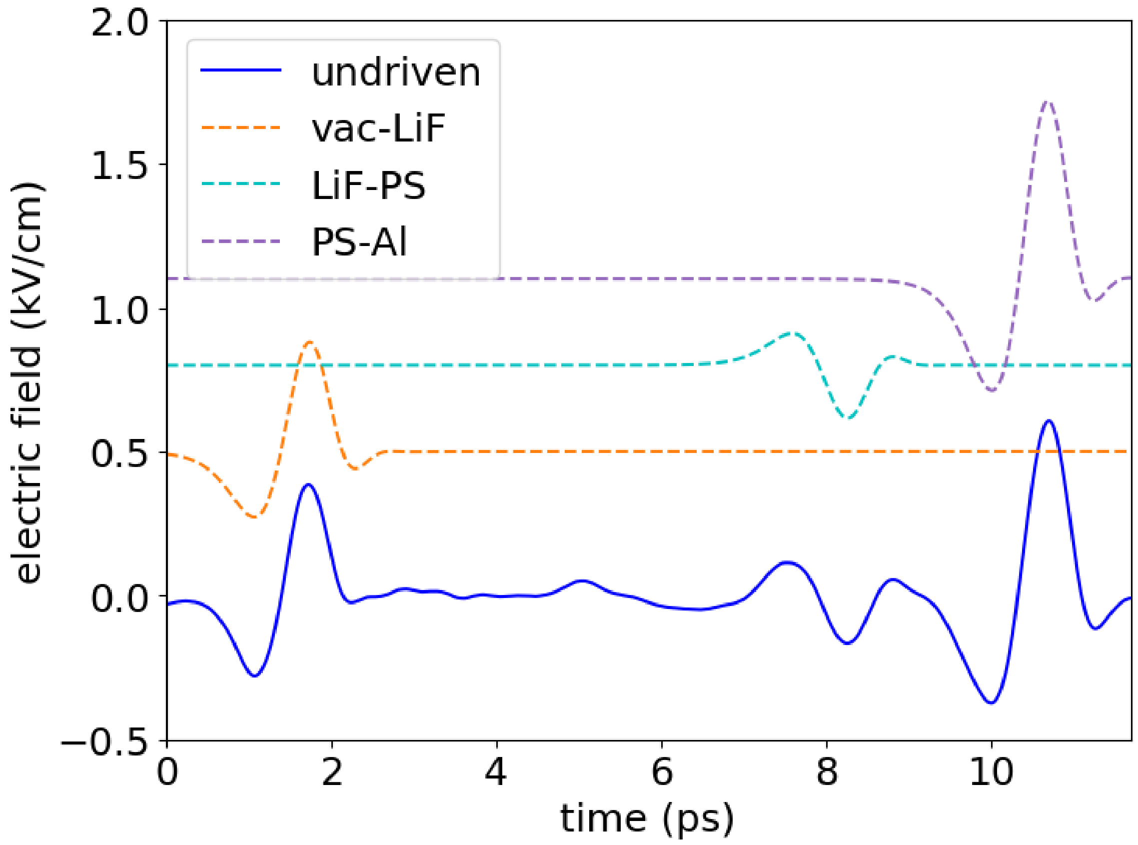

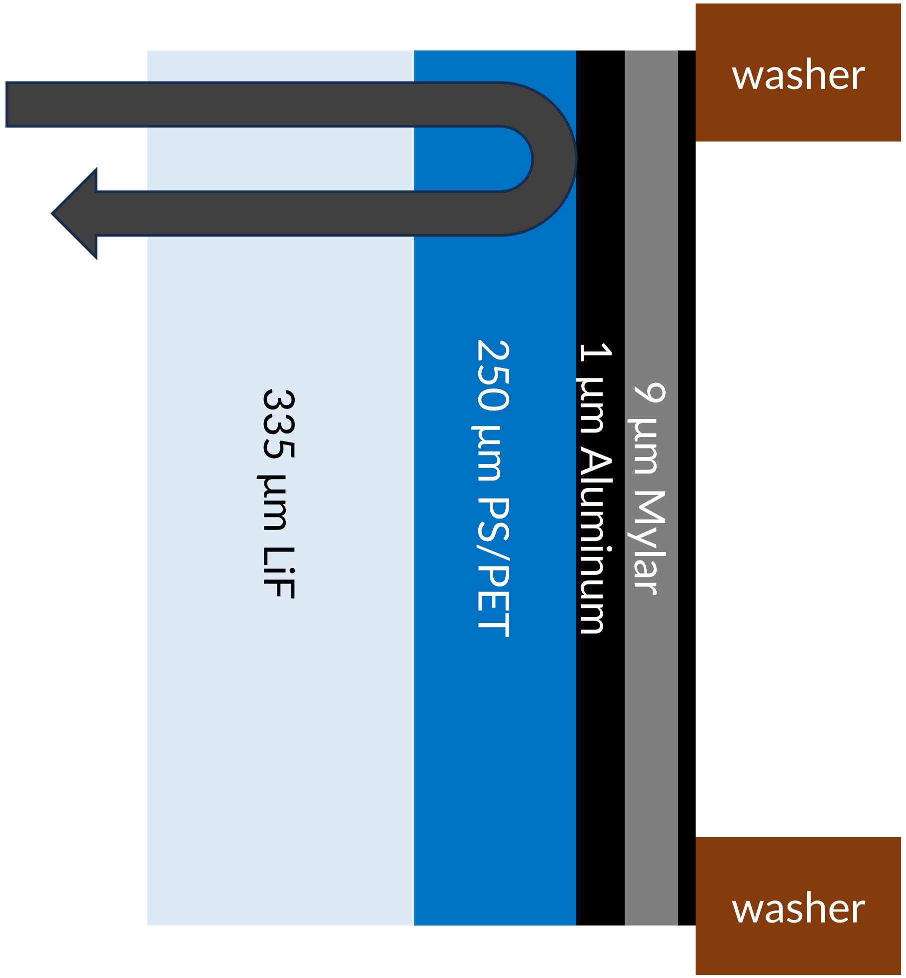

The time-domain waveform can be decomposed to extract contributions from the various pulses arising from reflections at different interfaces

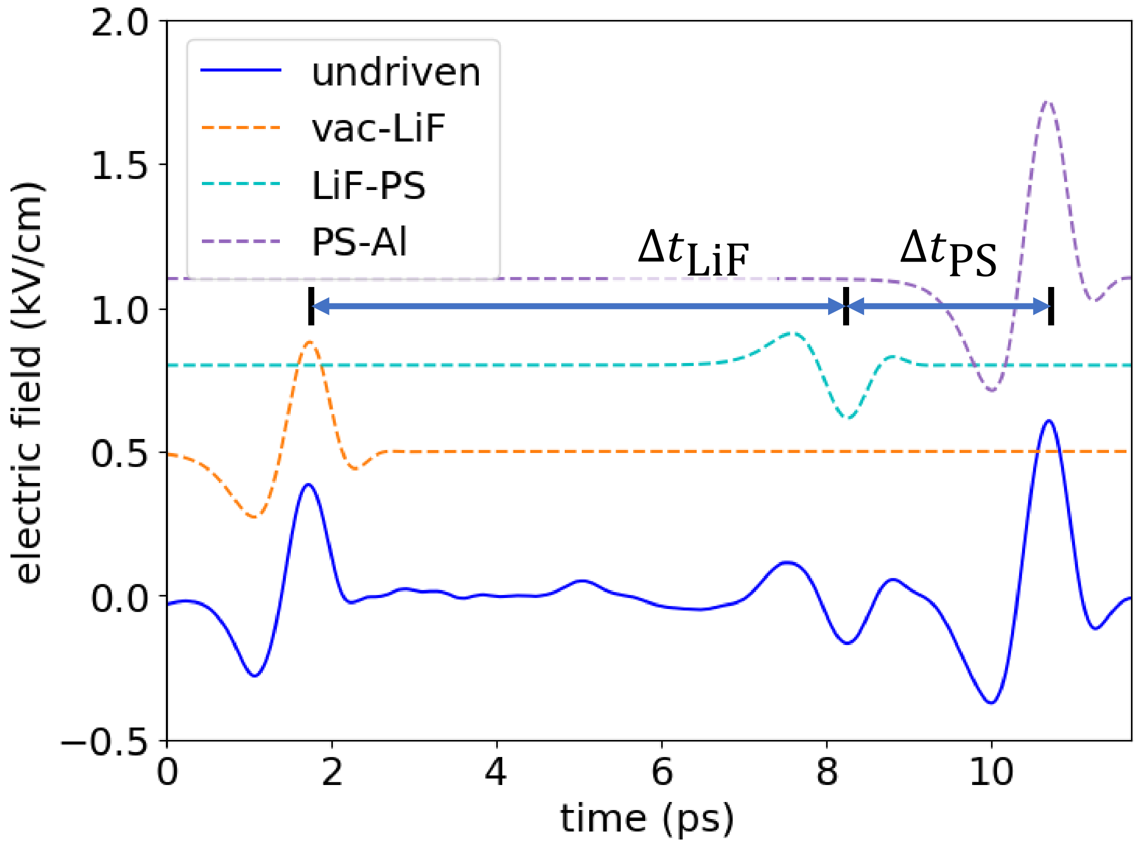

Polystyrene target assembly

Time delay between the pulses due to the optical path length of the layer: $\Delta t_j = \dfrac{2 n_j \Delta x_j}{c_0 \cos(\theta_j)}$

The time-domain waveform can be decomposed to extract contributions from the various pulses arising from reflections at different interfaces

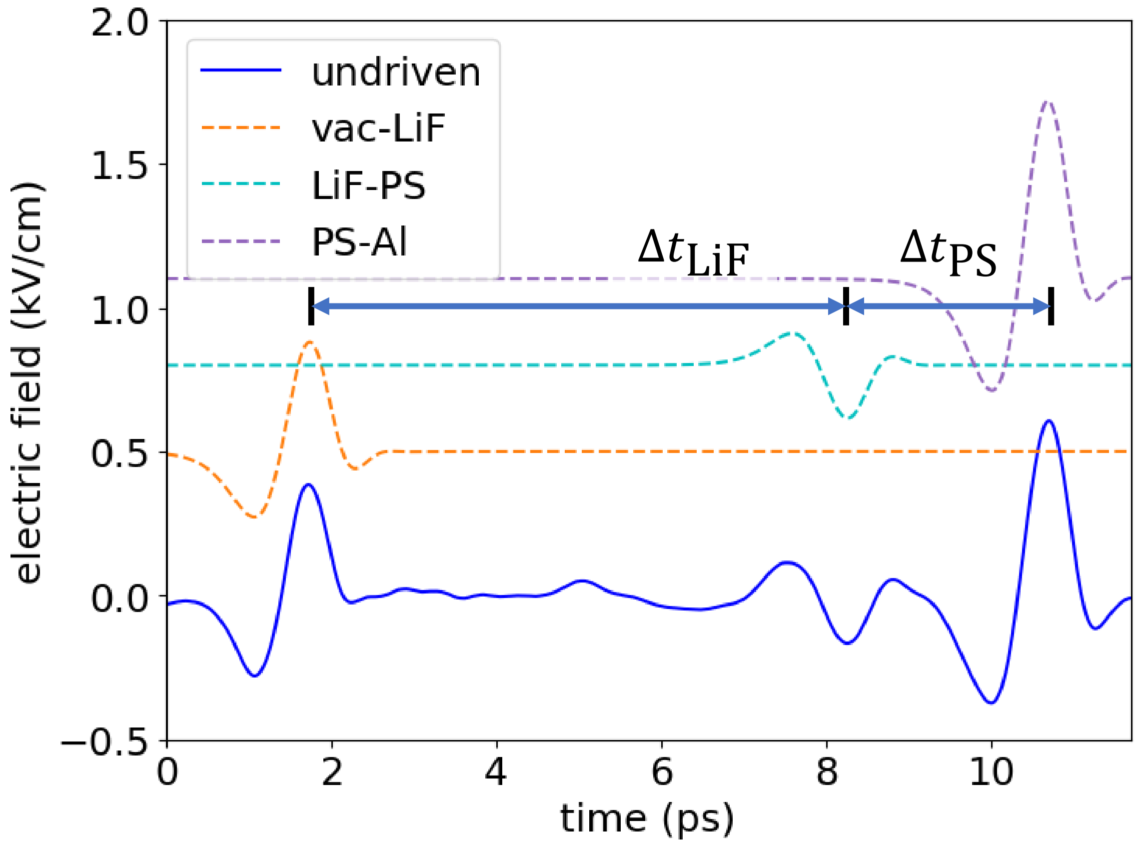

Polystyrene target assembly

Time delay between the pulses due to the optical path length of the layer: $$\Delta t_j = \frac{2 n_j \Delta x_j}{c_0 \cos(\theta_j)}$$

Given literature values for $\tilde{n}_{\mathrm{LiF}}$ and $\tilde{n}_{\mathrm{PS}}$ at THz frequencies, we can double check the thicknesses of these two layers:

	LiF thickness	PS thickness
Target specs	335 µm	250 µm
Extracted	349 µm	211 µm

THz reflectivity diagnostic can accurately measure characteristics of undriven target.

Upon compression, the time-domain waveform shows an additional THz pulse, indicating the appearance of a new interface between the plastic and the Al reflector

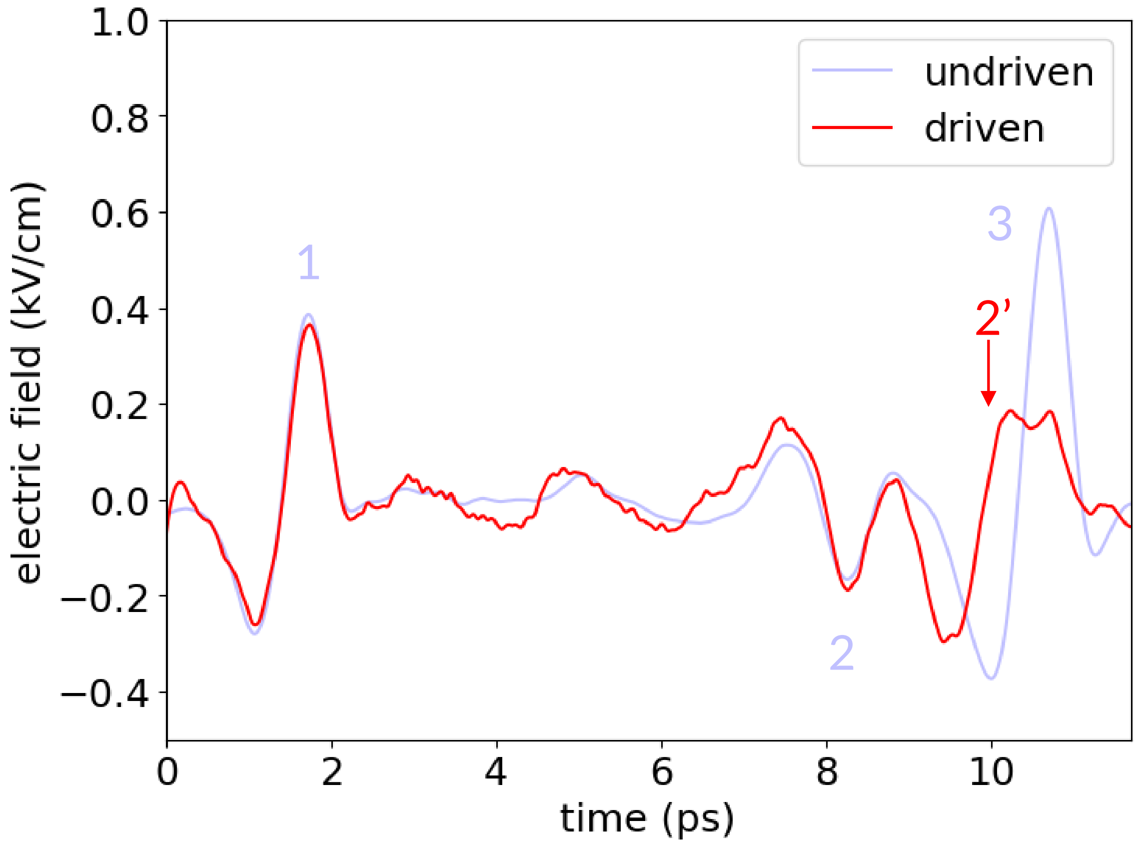

Polystyrene target assembly

Reflections occur when there is a significant change in the refractive index:

$$\tilde{r}_p = \frac{\tilde{n}_1 \cos(\theta_2) - \tilde{n}_2 \cos(\theta_1)}{\tilde{n}_1 \cos(\theta_2) + \tilde{n}_2 \cos(\theta_1)}$$

$\tilde{n}_1$= refractive index of layer 1
$\tilde{n}_2$= refractive index of layer 2

We observe reflections at:

1. vacuum-LiF interface
2. LiF-PS interface

2'. PS-shocked PS interface

3. PS-Al interface

Upon compression, the time-domain waveform shows an additional THz pulse, indicating the appearance of a new interface between the plastic and the Al reflector

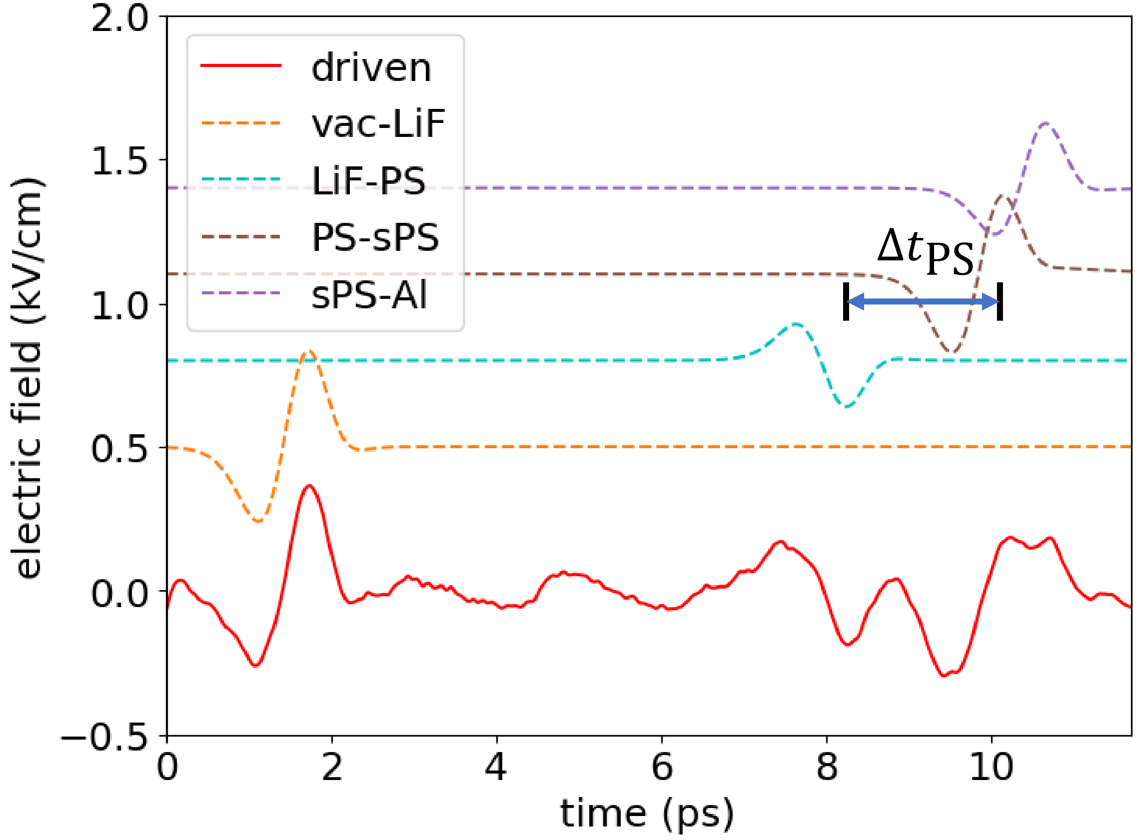

PS, U_s = 13.4 km/s, P ~ 110 GPa, T ~ 7000 K

THz pulse arrives 6.2 ns after shock enters PS layer
Δt_{PS}= 1.92 ps

	From VISAR	From THz data
% uncompressed	67%	65%

Changing the arrival time of the THz pulse compared with the shock breakout time supports the appearance of a moving interface within PS layer

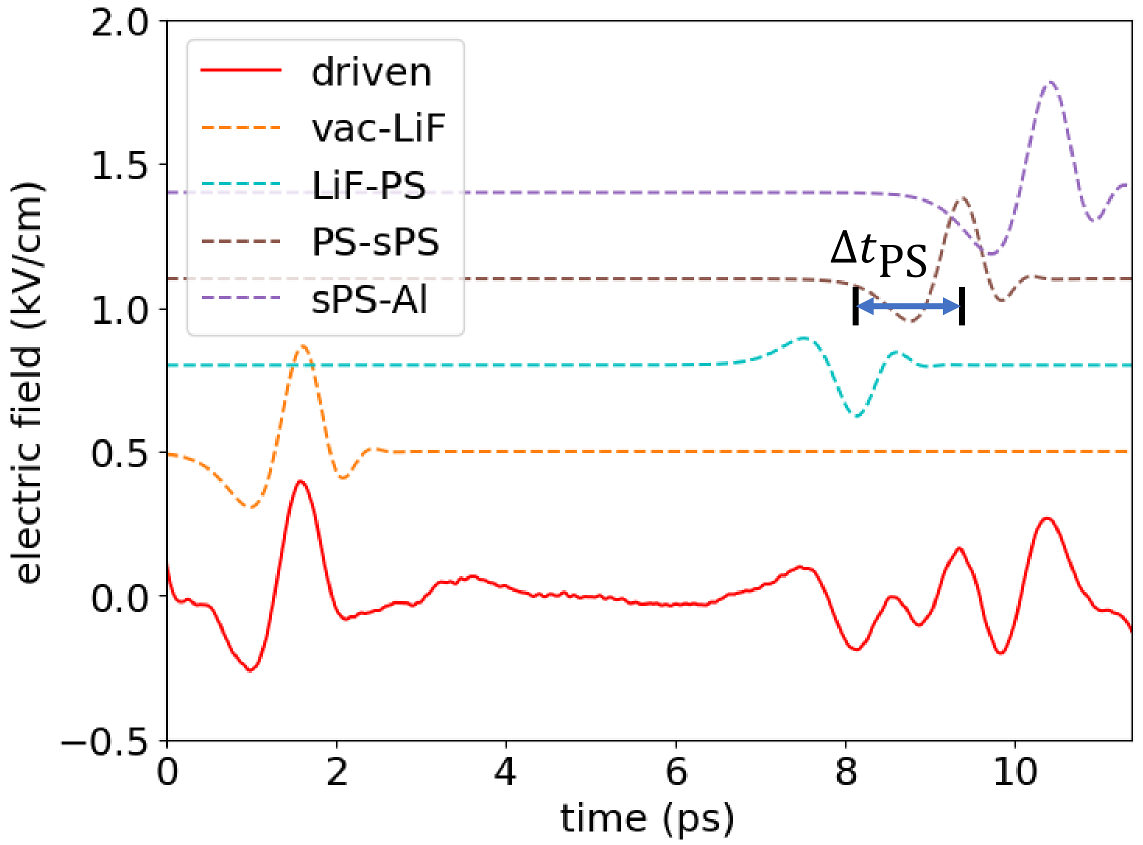

PS, U_s = 13.4 km/s, P ~ 110 GPa, T ~ 7000 K

THz pulse arrives 6.2 ns after shock enters PS layer
Δt_{PS}= 1.92 ps

	From VISAR	From THz data
% uncompressed	67%	65%

PS, U_s = 15.1 km/s, P ~ 144 GPa, T ~ 9700 K

THz pulse arrives 9.4 ns after shock enters PS layer
Δt_{PS}= 1.26 ps

	From VISAR	From THz data
% uncompressed	43%	44%

Regardless of shock strength, reflection from aluminum layer remains present, suggesting PS remains insulating.

In singly-shocked polystyrene, we do not observe enhanced conductivity upon compression.

Changing the arrival time of the THz pulse compared with the shock breakout time supports the appearance of a moving interface within PET layer

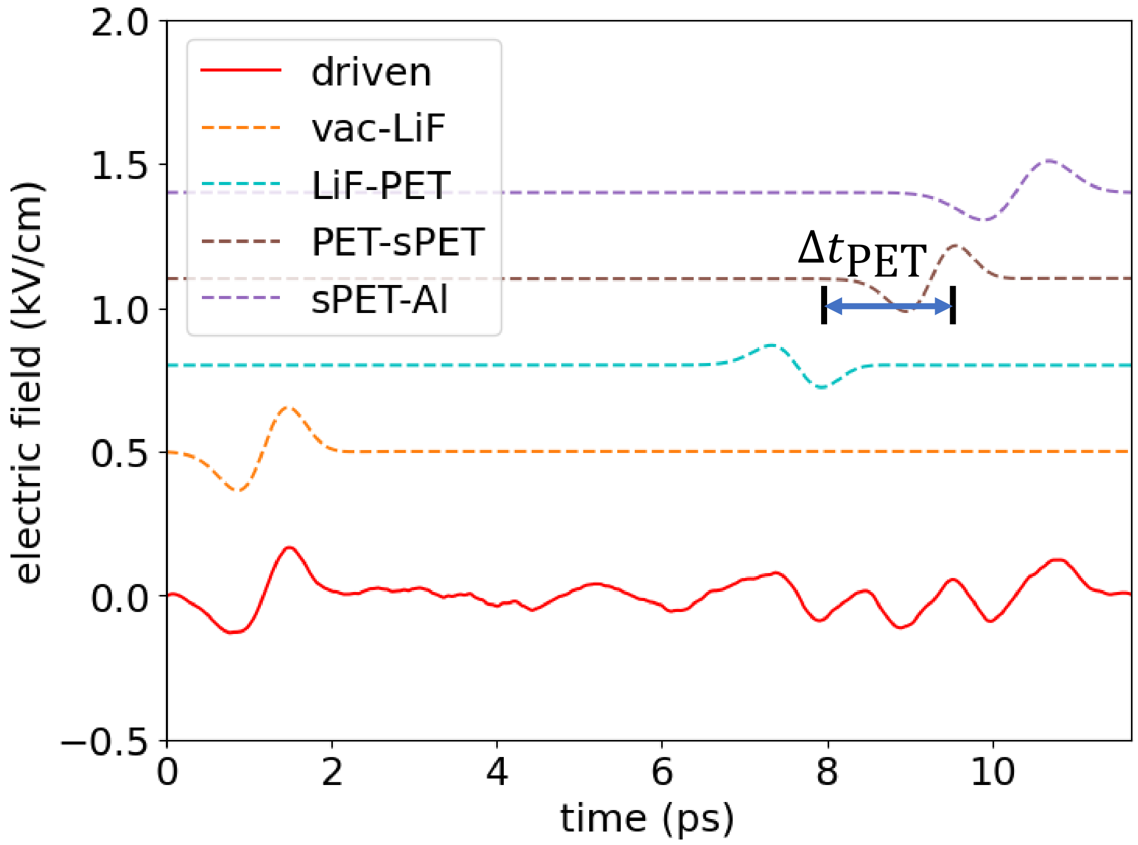

PET, U_s = 12.6 km/s, P ~ 126 GPa, T ~ 5830 K

THz pulse arrives 9.4 ns after shock enters PS layer
Δt_{PET}= 1.68 ps

	From VISAR	From THz data
% uncompressed	53%	56%

Regardless of shock strength, reflection from aluminum layer remains present, suggesting PET also remains insulating.

The pulses extracted from the time-domain waveforms can be used to infer the frequency-dependent refractive index of shocked plastic

Reflectivity

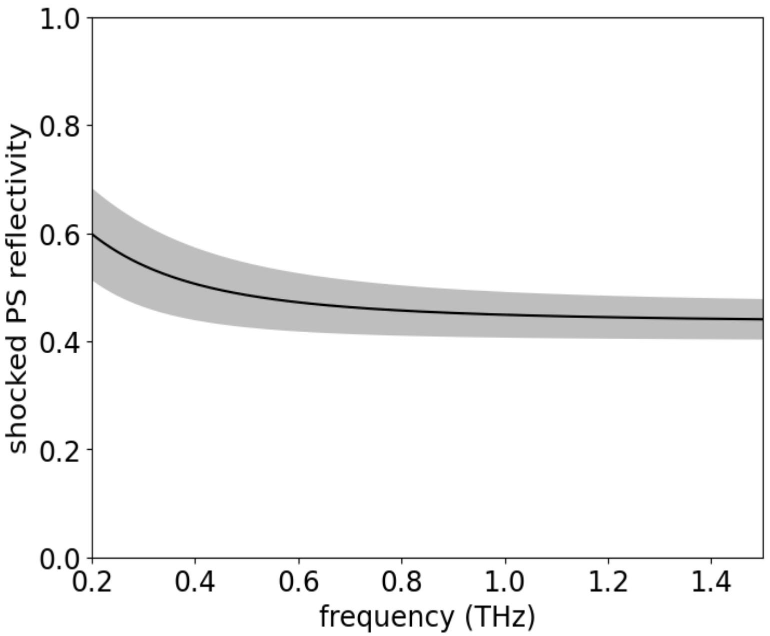

Refractive index

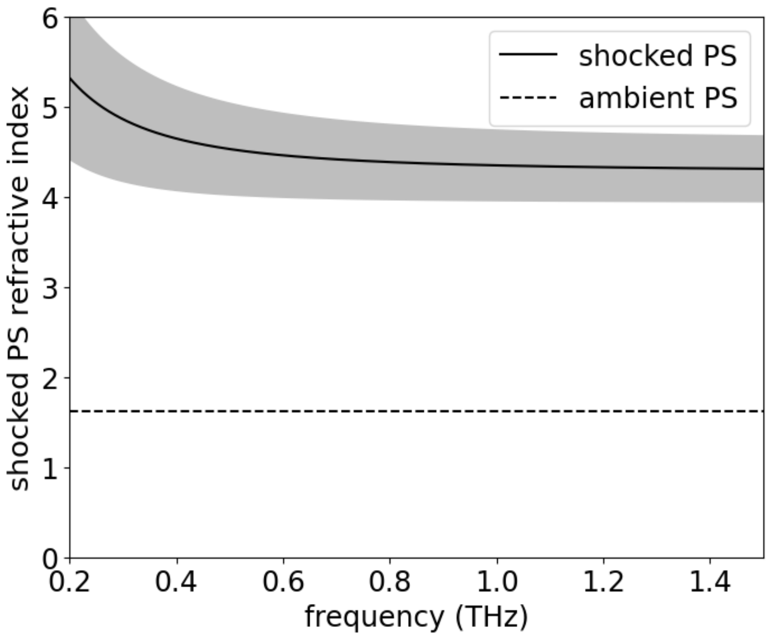

Constraints:

Reflections occur when there is a significant change in the refractive index:

$$\tilde{r}_p = \frac{\tilde{n}_1 \cos(\theta_2) - \tilde{n}_2 \cos(\theta_1)}{\tilde{n}_1 \cos(\theta_2) + \tilde{n}_2 \cos(\theta_1)}$$

Time delay between the pulses due to the optical path length of the layer:

$$\Delta t_j = \frac{2 n_j \Delta x}{c_0 \cos(\theta_j)}$$

Reflectivities and THz pulse delay times are used to determine the refractive index:

$$\tilde{n}^2(\omega) \approx n_0^2 + \frac{i\sigma}{\omega \epsilon_0}$$

We observe an increase in the refractive index when PS and PET are compressed

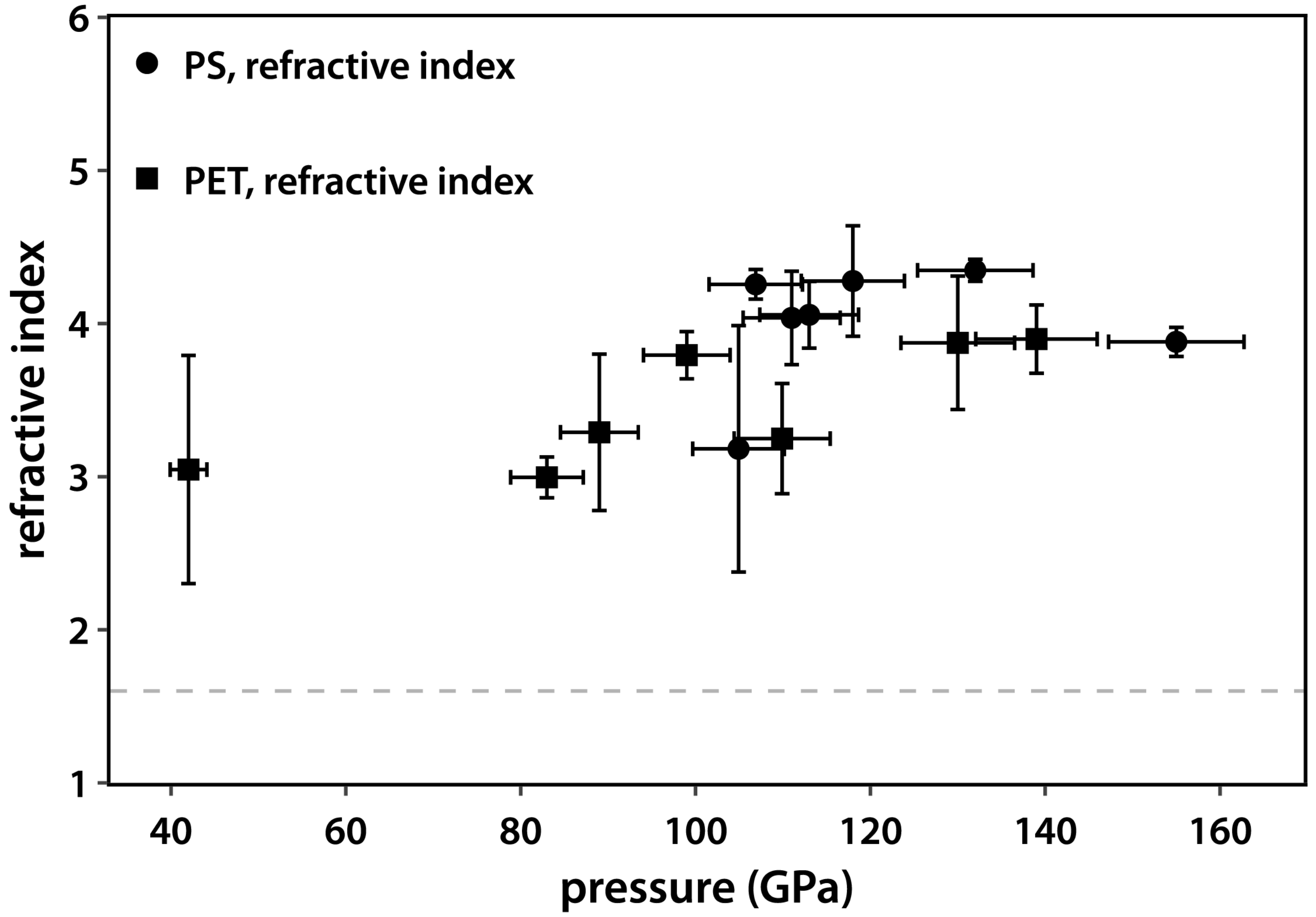

Observations:

- An increase in the refractive index when compressed

We observe an increase in the refractive index when PS and PET are compressed and can determine estimates of the conductivity from the THz data

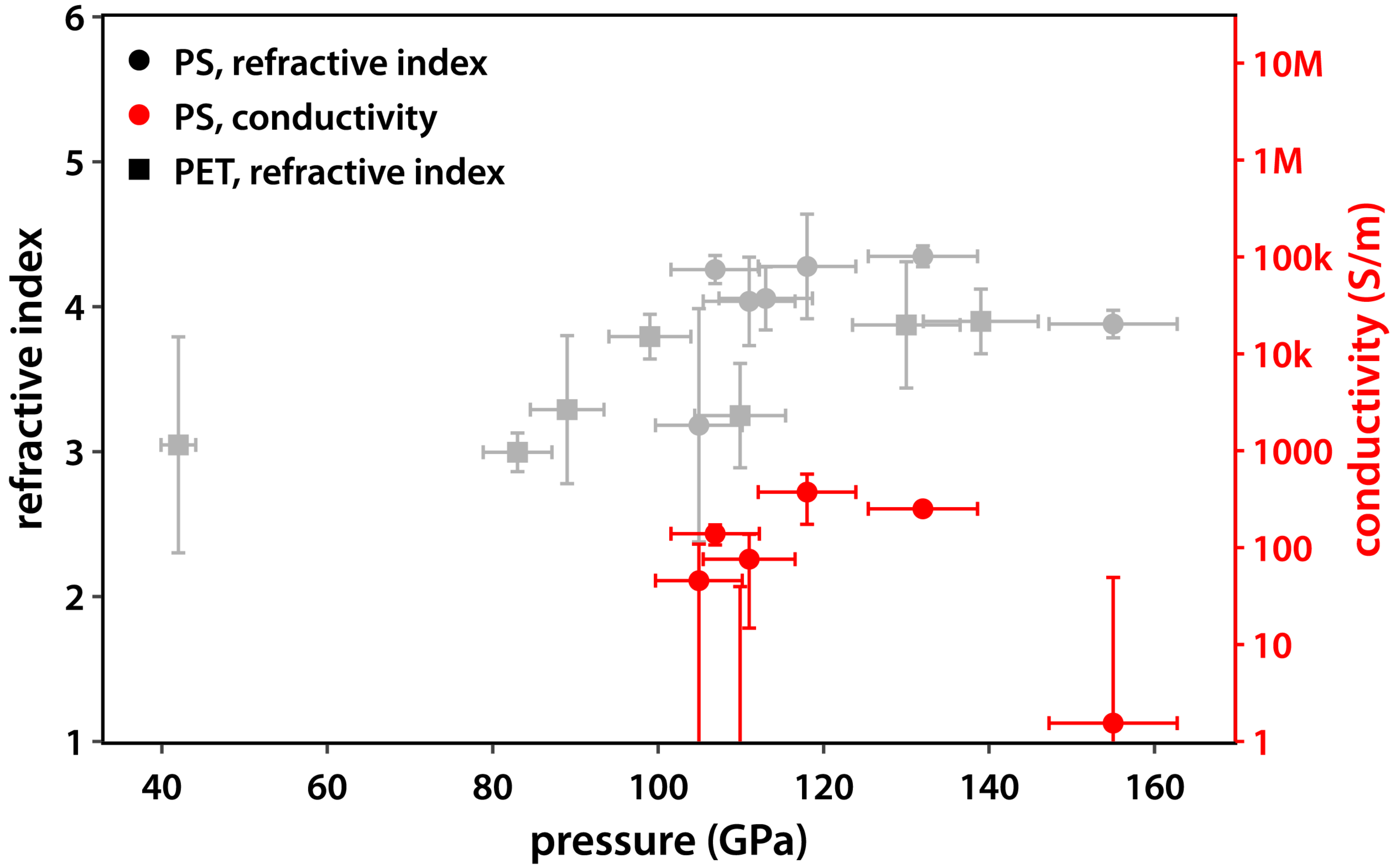

Observations:

- ➢ An increase in the refractive index when compressed
- ➢ Conductivity for compressed PS varies from 1-1000 S/m

We observe an increase in the refractive index when PS and PET are compressed and can determine estimates of the conductivity from the THz data

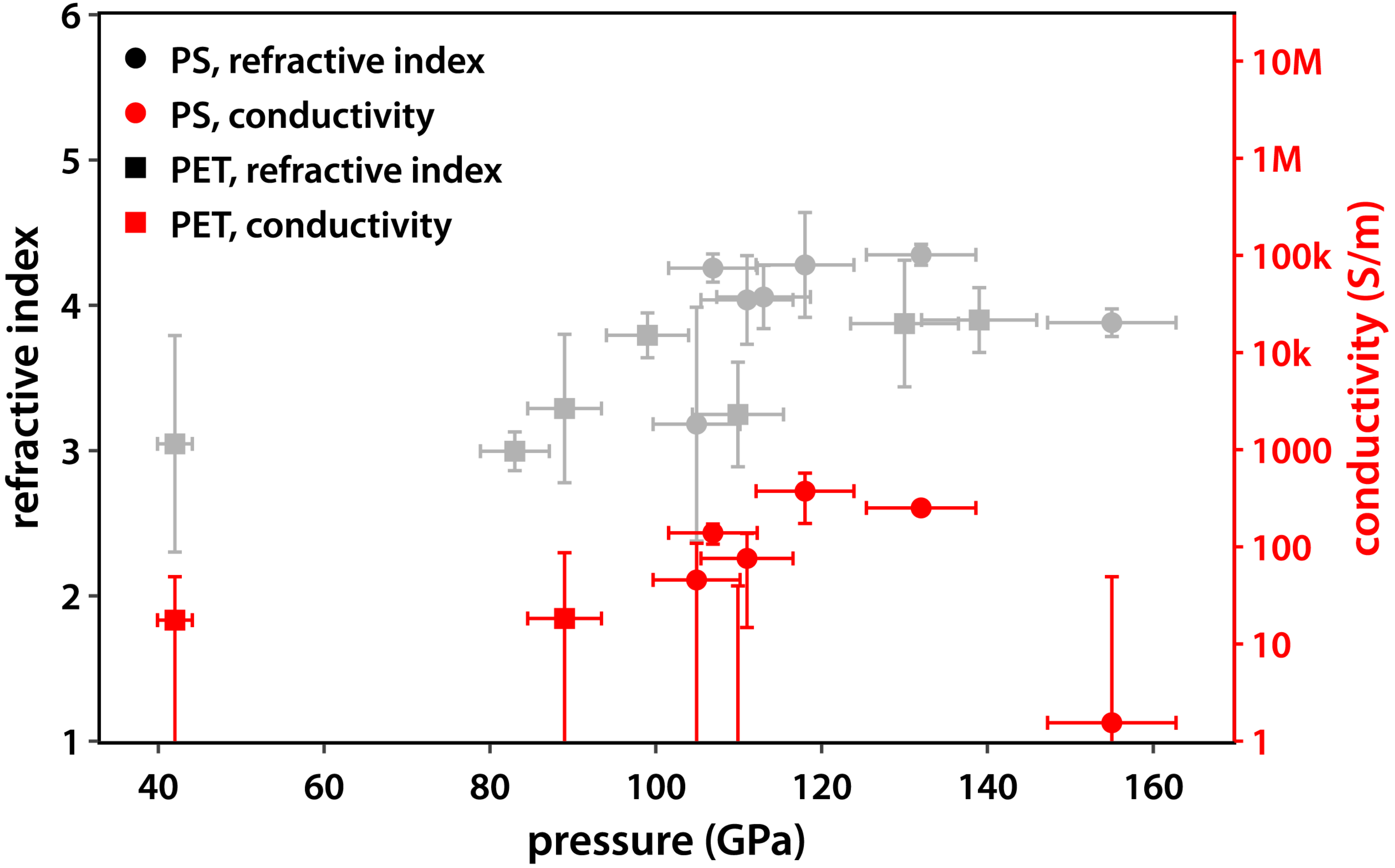

Observations:

- An increase in the refractive index when compressed
- Conductivity for compressed PS varies from 1-1000 S/m
- Conductivity for compressed PET similar to PS

We observe an increase in the refractive index when PS and PET are compressed and can determine estimates of the conductivity from the THz data

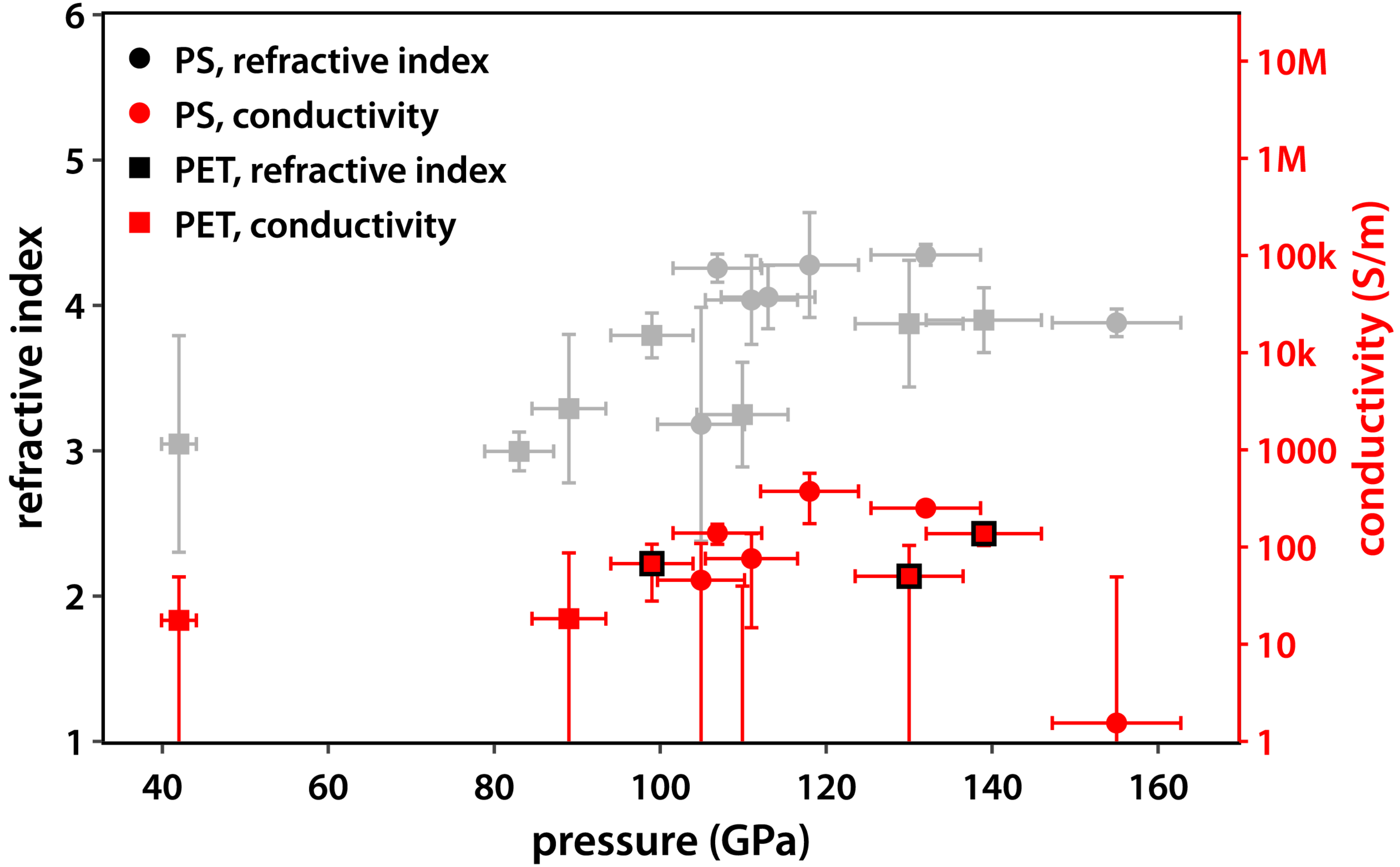

Observations:

- An increase in the refractive index when compressed
- Conductivity for compressed PS varies from 1-1000 S/m
- Conductivity for compressed PET similar to PS

No enhancement in electrical conductivity in regions where diamonds are expected to form.

Conclusions

Using THz spectroscopy, we have investigated the low-frequency electrical properties of warm dense hydrocarbons produced by dynamic compression.

We observe an increase in the refractive index of polystyrene and polyethylene terephthalate upon shock compression up to 155 GPa.

No enhancement of macroscopic conductivity is observed in regions where polyethylene terephthalate forms diamonds, suggesting metallic H_2 may form in nanoscale regions.

Acknowledgements

SLAC
E. R. Toro
L. B. Fletcher
S. H. Glenzer
B. K. Ofori-Okai

LLNL
S. J. Ali
T. M. Hutchinson
G. Righi

U. Rostock
P. T. May
D. Kraus

U. Michigan
S. Klein

U.S. DEPARTMENT OF ENERGY | Office of Science

LaserNetUS

DOE FES FWP100182
SLAC LDRD, under contract DE-AC02-76SF00515
DOE Contract No. DE-AC52-07NA27344
DOE FES Contract No. SCW 1836 “LaserNetUS: Discovery Science and Inertial Fusion Energy at the Jupiter Laser Facility”

Special thank you to the JLF staff!

Backup slides

Echelon-based single-shot THz spectroscopy

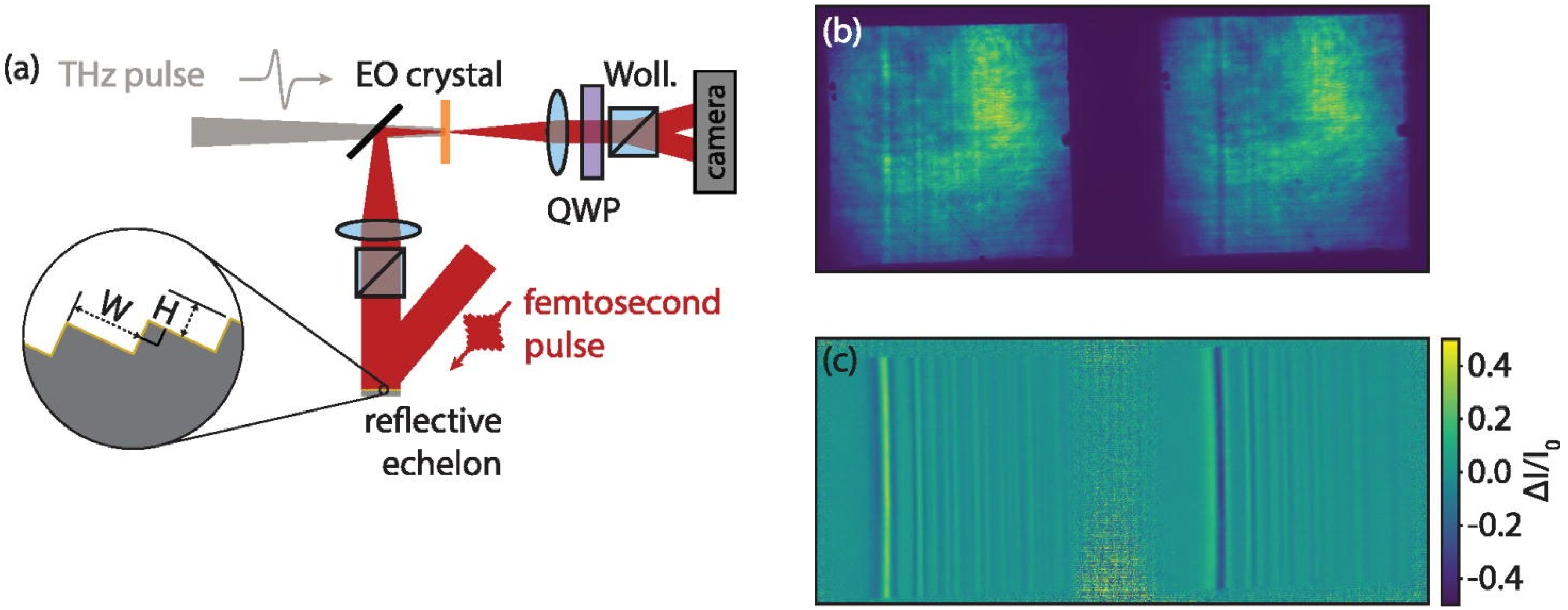

Ofori-Okai *et al.*, *Phys. of Plasmas* **31** 042711 (2024)